R. & M. No. 2678
(11,084, 11,191)
A.R.C. Technical Report

MINISTRY OF SUPPLY

AERONAUTICAL RESEARCH COUNCIL
REPORTS AND MEMORANDA

Measurements of Maximum Lift on 26 Aerofoil Sections at High Mach Number

Part I. Tests on 19 Aerofoils

By

J. A. BEAVAN, M.A., R. SARGENT, R. J. NORTH and Miss P. M. BURROWS

Part II. Tests on a Further 7 Aerofoils

By

R. J. NORTH and Miss P. M. BURROWS
of the Aerodynamics Division, N.P.L.

LONDON: HER MAJESTY'S STATIONERY OFFICE

1953

PRICE 8s. 6d. NET

Measurements of Maximum Lift on 26 Aerofoil Sections at High Mach Number

Part I. Tests on 19 Aerofoils

By

J. A. BEAVAN, M.A., R. SARGENT, R. J. NORTH and MISS P. M. BURROWS,
of the Aerodynamics Division, N.P.L.

*Reports and Memoranda No. 2678**
January, 1948

1. *Summary.*—The lift on a number of aerofoil sections mostly of 2-in. chord has been determined over a wide range of incidence and Mach number by measuring the pressures on the walls of the 20 × 8 in. High Speed Tunnel.†

There is some evidence that the low Reynolds number of the tests is not important and that the following general conclusions may be held to apply to the full-scale aeroplane.

(1) In almost every case, at Mach numbers above about 0·75 the lift *vs.* incidence curve comes to no definite maximum but is still rising at the limiting incidence of test (about 15 deg), though the rate of rise is much less above a certain incidence.

In the following conclusions, (2) to (5), the ' maximum lift ' at a given Mach number is defined by the first peak on the C_L/α curve, but for the higher Mach numbers where there is no maximum a dotted extension of the curves of $C_{L\,max}$ against M shows the lift at approximately the same incidence as that at which the last maximum was measured.

(2) For Mach numbers greater than 0·6, thin aerofoils have greater maximum lift than thick ones, whether symmetrical or cambered, of conventional or of low-drag design.

(3) In a similar range of Mach number, camber markedly increases the maximum lift; so much so that for example in cases where a symmetrical section shows a dropping off as M increases above 0·6, the corresponding cambered section may show a rise, before a drop at about 0·7.

(4) Somewhat scanty evidence seems to confirm the accepted idea that low-drag aerofoils (thickness position 40 to 50 per cent of the chord) have higher maximum lift above about $M = 0{\cdot}6$ than conventional shapes, but the difference is not great.

(5) At the highest speeds, above $M = 0{\cdot}7$, the effect of moving the maximum camber position from 40 to 60 per cent of the chord is an improvement of 0·04 on the Mach number at which $C_{L\,max}$ begins to fall, for a 12 per cent low drag aerofoil. An even greater improvement is found with a thicker conventional aerofoil for a change in maximum camber position from 20 to 40 per cent.

2. *Introduction.*—The known falling off of maximum lift at high Mach number is becoming a matter of considerable importance, but available data is scanty[1]. Hence it was thought worth while to undertake a quasi-systematic investigation by measuring up to high incidence the lift of a large number of aerofoils which have already been in use at the National Physical Laboratory.

* Published with the permission of the Director, National Physical Laboratory.

† The absolute values of lift given in this report may be subject to a correction of + 5 to + 10 per cent. (*See* section 3).

These aerofoils are nearly all of only 2-in. chord, which limits the Reynolds number to $0{\cdot}45$ to $0{\cdot}75 \times 10^6$ in these tests in the 20×8 in. High Speed Tunnel, operating at atmospheric pressure. But there is some evidence that comparisons between different shapes are applicable to full scale in the important range $M = 0{\cdot}5$ upwards.

3. *Method and Range of Tests.*—As the 20×8 in. High Speed Tunnel is not provided with a balance, the tests were carried out by the method of integrating the pressures read on the tunnel walls[2]. In the present instance these walls were set to give constant velocity along the tunnel in the absence of the aerofoil, at Mach numbers $0{\cdot}6$, $0{\cdot}7$, $0{\cdot}75$, $0{\cdot}8$, since the smallness of the aerofoil chord/tunnel width ratio (2 in./17·5 in.) did not justify the extra labour of using 'streamline walls '[2].

The difference of pressure between corresponding holes on the two sides of the tunnel (example Fig. 1) was integrated for a distance of approximately 14 in. up and downstream of the aerofoil, and a correction on the basis of an equivalent vortex at the aerofoil quarter chord was applied to allow for the residual pressure difference beyond. This is variable with Mach number, being about 7 per cent at $M = 0{\cdot}4$, and 2·2 per cent at $M = 0{\cdot}75$.

The general run of the results in relation to determinations elsewhere by other methods, together with further 5-in. chord tests by pressure plotting and simultaneous wall pressures, lead to the conclusion that although their comparative value is unimpaired, all lifts are underestimated, possibly to 5 to 10 per cent. It is now realized that this is probably due to loss of circulation at the ends of the aerofoil in the boundary layer (about $\frac{3}{4}$-in. thick) of the side walls of the tunnel.

It was not thought necessary in general to extend the incidence range far beyond the stall, when one occurred, or very far beyond the major kinks that were found in the lift curves in the absence of a stall. The highest angle was therefore about 14 deg, though one case (NL 1550/3050, Fig. 19) was pursued as far as 35 deg.

In general, the C_L peak characteristic of low Mach numbers changed at a Mach number within the range of observation to a continuous rise of C_L with incidence. It did not seem worth while to continue much beyond this critical speed, and the top speed of test was limited to $M = 0{\cdot}75$ or $0{\cdot}8$, though slightly higher speeds could usually have been obtained.

4. *Aerofoils.*—The following is a list of the aerofoils that have been tested*, together with a previously used notation[3] giving the major characteristics of the shape. In this notation 1730/2040 for example, denotes an aerofoil which has a maximum thickness 17 per cent of the chord at $0{\cdot}30c$ from the nose, and camber 2·0 per cent at $0{\cdot}40c$.

The aerofoils were all of 2 in. chord unless otherwise stated.

---

* The Tables include the aerofoils of Part II of this report.

TABLE 1

Type	Normal Description	Notation	L.E. Radius		½ T.E. Angle	½ T.E. Angle	Fig.
			ϱ/c per cent	$\frac{\varrho}{c}\Big/\left(\frac{t}{c}\right)^2$	deg	$100\ t/c$	
Conventional Sections	NACA 0012	N 1230	1·59	1·1	7·8	$0·6_5$	3
	NACA 0020	N 2030	4·40	1·1	12·8	$0·6_5$	4
	NACA 0020 1·2 in.	N 2030	4·40	1·1	12·8	$0·6_5$	5
	NACA 2417	N 1730/2040	3·19	1·1	10·9	$0·6_5$	6
	NACA 2218	N 1830/2020	3·56	1·1	11·3	$0·6_5$	7
	NACA 2218 5 in.	N 1830/2020	3·56	1·1	11·3	$0·6_5$	8
	Clark Y 7 per cent	CY 0733/1741	0·54	1·1	4·65	$0·6_5$	9
	Clark Y 15 per cent	CY 1533/4341	2·47	1·1	9·6	$0·6_5$	10
	RAF 69	R 2131/1944	2·0	0·5	8·5	0·4	11
NACA Low-drag Sections (16 series)	NACA 16/15*	NL 0650/1250	0·17	0·5	8·5	1·4	12
	NACA 16/21	NL 0750/3050	0·23	0·5	11·25	1·5	13
	NACA 16/12	NL 1050/1250	0·48	0·5	12·8	1·3	14
	NACA 16/22	NL 1050/3050	0·48	0·5	14·5	$1·4_5$	15
	NACA 16/32	NL 1050/4850	0·48	0·5	16·5	$1·6_5$	16
	NACA 16/16	NL 1550/1250	1·07	0·5	18·9	$1·2_5$	17
	NACA 16/26	NL 1550/3050	1·07	0·5	20·1	$1·3_5$	18, 19
	NACA 16/36	NL 1550/4850	1·07	0·5	20·5	$1·3_5$	20
Other Low-drag Sections	EC 1240	As normal description	0·90	0·6	10·7	0·9	21
	EC 1240/0640		0·90	0·6	10·7	0·9	22
	EC 1240/0658		0·90	0·6	10·7	0·9	23
	EC 1250		0·72	0·5	15·6	1·3	24
	EC 1250 5 in.		0·72	0·5	15·6	1·3	25
	EQH 1250/0640		0·72	0·5	12·3	1·0	26
	EQH 1250/1050		0·72	0·5	12·3	1·0	27
	EQH 1550		1·12	0·5	14·9	1·0	28
	EQH 1550/1058		1·12	0·5	14·9	1·0	29
	Piercy 20 per cent	P 2040	2·32	0·6	17·9	0·9	30
	Goldstein-Richards reflex	GR 1540/2037	1·32	0·6	7·7	0·5	31
	Biconvex $7\frac{1}{2}$ per cent	$07\frac{1}{2}50$	0	0	8·5	$1·1_5$	32

* N.P.L. Designation.

The various comparisons to show the effect mainly of changes of a single parameter of shape may be more clearly seen from the following table. In each section the camber increases downwards.

TABLE 2

	Maximum Thickness at:		
Thickness (per cent)	30 per cent	40 per cent	50 per cent
6 to 7½	CY 0733/1741		NL 0650/1250 NL 0750/3050 Biconvex 07½50
10			NL 1050/1250 NL 1050/3050 NL 1050/4850
12	N 1230	EC 1240 EC 1240/0640 EC 1240/0658	EC 1250 EQH 1250/0640 EQH 1250/1050
15	CY 1533/4341	GR 1540/2037	EQH 1550 EQH 1550/1058 NL 1550/1250 NL 1550/3050 NL 1550/4850
17 or 18	N 1730/2040 N 1830/2020		
20 or 21	N 2030 R 2131/1944	P 2040	

5. *Discussion of Results.*—The maximum lift for a given Mach number has been read off Figs. 3a-32a and plotted against Mach number in Figs. 3b-32b. In most cases, as has been stated, the C_L/α curves show no maximum above a certain speed. The curves of maximum lift, however, have been continued beyond this speed as a broken line extension giving the lift at the same incidence for which maximum lift occurred at a lower Mach number.

A second curve is also included in Figs. 3b to 32b to show the approximate C_L at which the lift or incidence curve begins to depart from its hitherto steady rise. This might be taken to indicate the earliest possible onset of buffeting troubles[4].

Further points are also included in the figures to show the highest C_L actually measured, although it is obvious that in nearly all cases this might have been increased indefinitely by going to higher incidence.

In Figs. 33 to 41 these results have been grouped in various ways as follows:

5.1. *Reynolds Number.*—The Reynolds number for tests with 2-in. chord aerofoils is small, ranging from 0·45 to 0·7 million for Mach number 0·4 to 0·75. It has been suggested[4] that in the range of interest, *i.e.*, high incidence and Mach number above about 0·5, this is not very important. The following few comparison tests seem to corroborate this assumption:

(1) The results (Fig. 33a) with NACA 0012, above $M = 0{\cdot}4$, agree well with the mean of a number of U.S.A. and German[1] results on the same section at a much higher Reynolds number (5×10^6).

(2) The strength of the standard 5-in. chord pressure-plotting models is not considered sufficient for high lift at high Mach number, but solid models of NACA 2218 and EC1250 exist and were tested for comparison with the similar 2-in. chord sections.

On EC1250 the lift values at low incidence at speeds below $M = 0{\cdot}7$ were not in good agreement, presumably due to Reynolds number effects in the sensitive part of the range of this low drag aerofoil*; but for incidence above about 8 deg Fig. 33b shows that the values of maximum lift do not differ unreasonably.

(3) In the case of the tests on the solid model of NACA 2218 (Fig. 8a) maxima on the C_L/α curves were not obtained at any speed, most probably due to the excessive blockage effects at high incidence with this thick (18 per cent) section. However, Fig. 33c shows that the fairly well defined values of C_L at which the lift curve begins to turn over agree well (above $M = 0{\cdot}55$) for the two sizes of aerofoil. The actual stall of the smaller aerofoil appears by Fig. 33c to be a guide at $M = 0{\cdot}5$ and $0{\cdot}6$ to the ' near-stall ' of the large chord tests.

(4) A smaller model, 1·2-in. chord, of NACA 0020 exists, and tests (Fig. 33b) compare fairly well with the 2-in. chord section.

5.2. *Thickness.*—Although the behaviour of the $C_{L\,\max}/M$ curve may be very different for different types of section, thicker aerofoils always have a lower maximum lift than the corresponding thin ones, in the upper part of the speed range. Fig. 34 compares aerofoils of varying thickness of (a) symmetrical conventional, (b) symmetrical low-drag, (c, d, e, f) cambered low-drag type.

In Fig. 34b it should be noted that a sharp-nosed thin aerofoil is compared with round-nosed thicker sections, the difference in the nose shape probably accounting for the lower $C_{L\,\max}$ of the former aerofoil at low Mach numbers.

It will be seen that the peaks, or rises, in the curves show a displacement in the direction of decreasing Mach number with increasing thickness for any family of aerofoils, which may be attributed to the higher local Mach numbers associated with increased curvature of the aerofoil surface. In cases where there are no peaks, such as with thick conventional sections, the same progressive displacement may be noted in the Mach number at which the $C_{L\,\max}$ begins to decline rapidly.

5.3. *Thickness Position.*—The present series of aerofoils does not provide very satisfactory comparisons to show the effect of altering the thickness position only. The best that can be done seems to be:

(1) For symmetrical thick aerofoils the Piercy section with thickness 20 per cent at 40 per cent back is superior to the conventional NACA 0020 above a Mach number of about $0{\cdot}55$, the gain in Mach number for the same maximum lift being of the order $0{\cdot}04$ (Fig. 39a).

(2) For symmetrical medium thin aerofoils EC1250 is better than EC1240 (Fig. 39b). The latter differs little from the conventional NACA 0012, which, however, has a different design of nose.

(3) The only strict comparison of cambered sections (Fig. 39c) shows that EQH1250/0640 with further back thickness has a *lower* maximum lift than EC1240/0640.

The conclusion seems to be that existing evidence agrees in the main with the accepted view that low-drag aerofoils are somewhat better than those with maximum thickness at the conventional 30 per cent of the chord.

* Peculiarities in the behaviour of this aerofoil, due to the very flat pressure distribution and the very large trailing edge angle, are discussed in R. & M. 2065[10]. They would certainly be expected to lead to variation in transition and separation position with Reynolds number; but not when shock-waves exist near the leading edge, as at high incidence.

5.4. *Camber.*—There seems no doubt that camber is a major factor as regards maximum lift at high speeds, even a small amount in some cases having a marked beneficial effect. This is shown in Fig. 35c where a camber of only 0·6 per cent has raised the maximum lift of the EC1240 section by about 30 per cent at $M = 0{\cdot}7$.

The effect on similar 12 per cent thick sections with maximum thickness even further back (at mid-chord), seems smaller (Fig. 35d). But at about 7, 10 and 15 per cent thickness the NACA 16 series aerofoils NL in Figs. 35a, b, e show a steady increase with camber (the NACA 16 series sections are of a very similar type to EQH1550, having nearly elliptical noses and blunt tails; and in fact the symmetrical NACA 16-015 would be nearly identical with EQH1550). The peaks of the curves show a displacement towards lower Mach numbers for increasing camber, in much the same way as for increasing thickness (section 5.2) and presumably for the same reason.

Three other low-drag aerofoils, with maximum thickness less far back, are compared in Fig. 35f. The data for the *Brabazon* 1 wing root section was obtained from R. & M. 2617[12]. There can be no rigid comparison between the three aerofoils but the effect of camber on thick sections is seen to be similar to that for other, thinner sections of the low-drag type.

Fig. 35g shows the relative merits of four typical thick conventional sections. Again, although no direct comparison can be made, the improvement with camber is noticeable. The 15 per cent Clark Y shows a superior $C_{L\,\max}$ at all Mach numbers, but this must be attributed to its comparative thinness. The collapse of $C_{L\,\max}$ at high Mach numbers is characteristic of thick conventional sections, and the advantage of low-drag sections in this respect may be noted by comparing Figs. 35f and g at $M = 0{\cdot}6$ for example.

The advantage of camber is strikingly shown in Fig. 36 where the values of $C_{L\,\max}$ at $M = 0{\cdot}6$ are plotted against percentage camber, irrespective of thickness ratio. A straight line may be drawn near all the points except for NACA 2218 (which is the only aerofoil with maximum camber outside the range of 37 to 58 per cent chord), Clark Y 15 per cent, with its flat under surface, and the thick NACA 0020 and RAF 69. Thickness has an overriding effect at higher Mach number, but it will be seen from Fig. 37 that the same tendency for camber to increase the maximum lift is shown at $M = 0{\cdot}75$ where an increase of about 0·1 in $C_{L\,\max}$ for 1 per cent increase of camber may be seen to apply to the aerofoils of thickness 15 per cent or less. The beneficial effect can also be seen by comparing individual C_L/α curves, as has been done for $M = 0{\cdot}75$ in Fig. 38.

5.5. *Camber Position.*—There are available two fairly strict comparisons of altered maximum camber position which agree in showing an improvement due to rearward movement.

With a low-drag section of basic shape EC1240 (Fig. 40b) displacement of maximum camber position from 40 to 58 per cent of the chord can be regarded as giving an improvement of 0·04 in Mach number for M above 0·65.

The conventional NACA 2417 (camber at 40 per cent) is markedly better than NACA 2218 (camber at 20 per cent) although a little of the improvement is probably due to the slight decrease of thickness, 18 to 17 per cent (Fig. 40a).

If the effect of a change of thickness position from 40 to 50 per cent is disregarded, comparison in Fig. 40c of GR1540/2037 with an interpolated NL1550/2050 (from Fig. 35) shows also a decided improvement with the further back camber.

5.6. *Camber and Thickness.*—Figs. 41a and b show cases where camber and thickness are varied proportionally. Two Clark Y aerofoils, 7 per cent and 15 per cent, are shown in Fig. 41a, and two similarly related aerofoils of the NACA 16 series in Fig. 41b. The thinner and less cambered sections both display lower $C_{L\,\max}$ than the thicker sections up to a fairly high Mach number, when the positions are reversed. But it is noticeable that the thinner sections show much less variation from the low speed value of $C_{L\,\max}$.

5.7. *Nose Radius.*—The shape of the nose, very important at low speed, is of great interest when shock-waves may be present near the leading edge (*i.e.*, at high incidence). But unfortunately no comparisons are possible that do not involve alteration of other parameters of the shape. It will be realised that alterations of the bluntness of the nose are associated with the change of the position and magnitude of maximum thickness, for example in comparing EC 1240 and EC1250, or NACA 0012 and NACA 0020. The values of nose radius ϱ in Table 1 nearly all give approximately $(\varrho/c)(t/c)^2 = 1{\cdot}1$, $0{\cdot}6$ and $0{\cdot}5$ respectively for aerofoils with maximum thickness at 30, 40 and 50 per cent.

5.8. *Trailing-Edge Angle.*—Most of the aerofoils discussed here have rather large trailing-edge angles (*see* Table 1), but it might perhaps be expected that at maximum lift, with considerable shock-waves already present near the nose, the influence of the tail would not be very important.

5.9. *General.*—Little will be added here to the detailed discussion of high-speed effects on lift at high incidence in terms of pressure distribution given in Refs. 1 and 4, the former of which is mainly a review of previous work. But a further survey of relevant information (up to Dec. 1947), and some attempt to explain certain of the effects on the basis of pressure-plotting results at high M[4–10], is included in Ref. 11.

It is regretted that the present series of measurements, undertaken with the specific object of obtaining as much information on actual values as possible, could not include other observations—shock-wave positions*, separation (by wool tufts)—without greatly adding to the time and labour of the tests. It is felt that such work should be combined with pressure plotting and that the present results may help towards deciding the best choice of aerofoils if an investigation is to be made.

6. *Conclusions.*—Conclusions to be drawn from the above discussion of the results are given in the Summary at the beginning of this report.

7. *Acknowledgements.*—A considerable amount of the work, both computational and observational, was carried out by other members of the High Speed Tunnel staff, notably Misses Faber and White.

* The aerofoils were not mounted in the glass walls of the tunnel.

Part II. Tests on a Further 7 Aerofoils

By

R. J. NORTH and MISS P. M. BURROWS

---

1. *Summary.*—The lift on a further seven 2-in. chord aerofoils has been determined over a range of incidence and Mach number by measuring the pressures on the walls of the 20 × 8 in. High Speed Tunnel.

The results are correlated with those of Part I of this report and show that the general beneficial effects of reducing thickness and increasing camber extend down to thicknesses of the order of 6 and 7 per cent.

In addition, the tests on NACA 0012 have been pursued to higher Mach numbers.

2. *Introduction.*—A list of the aerofoils tested, all of 2-in. chord, is given in Table 1 together with a notation expressing the chief geometrical characteristics of the section. There are four thin, and three thick, aerofoils, variously cambered, all related in some respect to aerofoils in the previous report. In Table 2 the sections are arranged to show the possible comparisons of the effect of changing a single parameter.

The experimental conditions and methods were similar to those of Part I. The deflection of the aerofoils at high Mach numbers and high lift-coefficients limited the maximum incidence for thin aerofoils.

3. *Discussion of Results.*—The general observations in Part I on the shape of the C_L/α curves and the effect of Reynolds number apply equally to this. It should be noted that, particularly with the thin sections, there are often considerable changes in slope before the stall, for example, the $7\frac{1}{2}$ per cent biconvex aerofoil at $M > 0{\cdot}725$ (Fig. 32a). Thus the $C_{L\,\max}/M$ curves may be optimistic at the higher Mach numbers regarded as a criterion to determine the highest useful lift coefficients[2].

3.1. *Thickness.*—The examples of the effect of thickness afforded by the further comparisons now possible confirm the advantage of thinness (Fig. 34b, d, e, f), which extends to the thinnest sections (6 and 7 per cent) tested. In Fig. 34b it should be noted that a sharp-nosed thin aerofoil is compared with round-nosed thicker sections, the difference in the nose shape probably accounting for the lower $C_{L\,\max}$ of the former aerofoil at low Mach numbers.

Also it will be seen here and in Fig. 34a and c that the peaks, or rises, on the curves show a displacement in the direction of decreasing Mach number with increasing thickness for any family of aerofoils, which may be attributed to the higher local Mach numbers associated with increased curvature of the aerofoil surface. In cases where there are no peaks, such as with thick conventional sections, the same progressive displacement may be noted in the Mach number at which the $C_{L\,\max}$ begins to decline rapidly.

3.2. *Camber.*—The steady increase of $C_{L\,\max}$ with camber for a series of thin aerofoils is well shown in Fig. 35a. The peak for Clark Y 7 per cent occurs at a lower Mach number than for any of the other sections, probably because the positions of maximum thickness and camber are further forward on this aerofoil.

The effect of camber on the 15 per cent NACA 16 series aerofoils is shown in Fig. 35e. This figure may be compared with Fig. 35a and b. It is evident that the beneficial effect of camber on $C_{L\,max}$ is maintained for thick and thin aerofoils of the series. The peaks of the curves show a displacement towards lower Mach numbers for increasing camber, in much the same way as the peaks are displaced for increasing thickness and presumably for the same reason. In the case of aerofoils which do not show a peak, the Mach number at which the $C_{L\,max}$ begins to fall off rapidly shows a similar progression with camber, as with thickness.

Three other low-drag aerofoils, with maximum thickness less far back are compared in Fig. 35f. The data for the *Brabazon* 1 wing root section was obtained from R. & M. 2617[12] There can be no rigid comparison between the three aerofoils but the effect of camber on thick sections is seen to be similar to that for other, thinner sections of the low-drag type.

Fig. 35g shows the relative merits of four typical thick conventional sections. Again, although no direct comparison can be made the improvement with camber is noticeable. The 15 per cent Clark Y shows a superior $C_{L\,max}$ at all Mach numbers but this must be attributed partly to its comparative thinness. The collapse of $C_{L\,max}$ at high Mach numbers is characteristic of thick conventional sections and the advantage of low-drag sections in this respect may be noted by comparing Fig. 35f and g, at $M = 0{\cdot}6$ for example.

As an extension of the method of presentation of Fig. 36, Fig. 37 was drawn using the results available from both Parts at $M = 0{\cdot}75$. It shows the effect of camber and thickness at high Mach numbers, clearly and simply. The increase of $C_{L\,max}$ with camber appears to be linear for small amounts of camber and the slope is approximately the same as that given by the results at $M = 0{\cdot}6$ and $M = 0{\cdot}7$. At the lower Mach numbers, however, the effect of thickness was much less noticeable and the stratification, remarkable at $M = 0{\cdot}75$, is not very clearly defined at $M = 0{\cdot}7$. The single point for a thickness of 20 per cent in Fig. 37 is explained by the fact that, in general, thick aerofoils did not show a definite $C_{L\,max}$ at $M = 0{\cdot}75$.

3.3. *Camber and Thickness.*—Figs. 41a, b show cases where camber and thickness are varied proportionally. Two Clark Y aerofoils, 7 and 15 per cent, are shown in Fig. 41a and two similarly related aerofoils of the NACA 16 series in Fig. 41b. The thinner and less cambered sections both display lower $C_{L\,max}$ than the thicker sections up to a fairly high Mach number, when the positions are reversed. But it is notable that the thinner sections show much less variation from the low-speed value of $C_{L\,max}$.

3.4. *NACA* 0012.—The tests on NACA 0012 have been pursued to higher Mach numbers than were undertaken for Part I and the complete results are given in Figs. 3a and b. The lift coefficient curve for $M = 0{\cdot}8$ has been revised in the light of the further observations. It is noteworthy that this aerofoil does not show a negative lift slope at high Mach number as NACA 0020 does (*see* Fig. 4a).

REFERENCES

No.	Author	Title, etc.
1	F. R. Kirk	Effects of Mach number on Maximum Lift. A.R.C. Report 10,463. January, 1947. (Unpublished.)
2	N. C. H. Lock and J. A. Beavan ..	Tunnel Interference at Compressibility Speeds using the Flexible Walls of the Rectangular High Speed Tunnel. R. & M. 2005. September, 1944.
3	W. F. Hilton	An Experimental Analysis of the Forces of eighteen Aerofoils at High Speeds. R. & M. 2058. May, 1946.
4	J. R. Spreiter and P. J. Steffen ..	Effect of Mach and Reynolds Numbers on Maximum Lift Coefficients N.A.C.A. Tech. Note 1044. March, 1946.
5	G. C. Furlong and G. Fitzpatrick	Effects of Mach and Reynolds numbers on Maximum Lift Coefficient of a 230-series Wing Section. N.A.C.A. Tech. Note 1299. May, 1947.
6	B. Göthert	*See* Guide to German Aerofoil Tests in the High Speed Tunnel of the DVL Berlin—J. R. Sutton. A.R.C. Report 10,918. June, 1947. (Unpublished.)
7	J. A. Beavan and G. A. M. Hyde ..	Pressure Distributions at High Speed on EC1250. (Data Report.) R. & M. 2625. July, 1947.
8	H. H. Pearcey and J. A. Beavan ..	Force and Pressure Coefficients up to Mach number 0·87 on the Goldstein Roof Top Section 1442/1547. R. & M. 2346. April, 1946.
9	E. W. E. Rogers and C. White ..	Force and Pressure Measurements up to Mach number 0·88 on a 10 per cent Modified NACA 16 series Propellor Section. A.R.C. Report 11,114.
10	J. A. Beaven, G. A. M. Hyde and R. G. Fowler	Pressure and Wake Measurements up to Mach number 0·85 on an EC1250 Section with 25 per cent control. R. & M. 2065. February, 1945.
11	J. A. Beavan and R. Hills ..	$C_{L\,max}$ of Aerofoil Sections at High Subsonic Mach number. A.R.C. Report 11,102. December, 1947. (Unpublished.)
12	A. B. Haines and W. Port	Pressure Plotting Tests in the R.A.E. High Speed Tunnel on a 21 per cent thick, low-drag Aerofoil (Brabazon I wing root section). R. & M. 2617. October, 1947.
13	D. J. Graham	High Speed Tests of an Aerofoil Section Cambered to have Critical Mach numbers higher than those obtainable with a Uniform-load Mean Line. N.A.C.A. Tech. Note 1396. August, 1947.

TABLE 1

Type	Normal Description	British Notation	L.E. Radius		T.E. Angle		Fig.
			$\frac{\varrho}{c}$	$\frac{\varrho}{c}\Big/\left(\frac{t}{c}\right)^2$	$\frac{1}{2}$ T.E. Angle	$\frac{\frac{1}{2}\text{ T.E. Angle}}{100\ t/c}$	
	Biconvex 7½ per cent	07½50	—	—	8·5	1·13	1
NACA Low-drag Propeller Sections	NACA 16/15	NL 0650/1250	0·17	0·5	8·5	1·42	2
	NACA 16/21	NL 0750/3050	0·23	0·5	11·25	1·50	3
	NACA 16/36	NL 1550/4850	1·05	0·5	20·5	1·37	4
Conventional Sections	Clark Y 7 per cent	CY 0733/1741	0·54	1·1	4·65	0·67	5
	Clark Y 15 per cent	CY 1533/4341	2·47	1·1	9·6	0·64	6
	RAF 69	R 2131/1944	2·0	0·5	8·5	0·41	7

TABLE 2

Maximum Thickness (per cent)	Maximum Thickness at		
	30 per cent	40 per cent	50 per cent
6–7½	CY 0733/1741	—	NL 0650/1250 NL 0750/3050 Biconvex 07½50
15	CY 1533/4341	—	NL 1550/4850
21	R 2131/1944	—	—

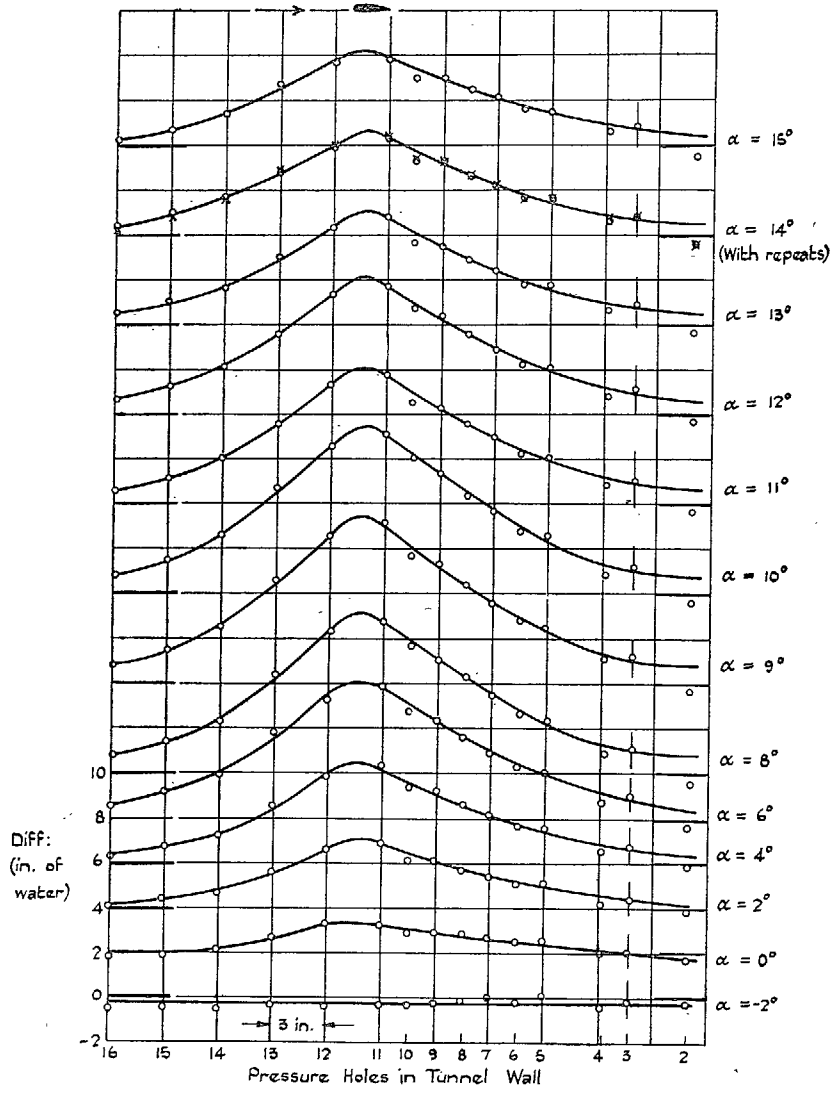

FIG. 1. Typical wall pressures (difference between the two sides), NACA 2218, $M = 0{\cdot}5$.

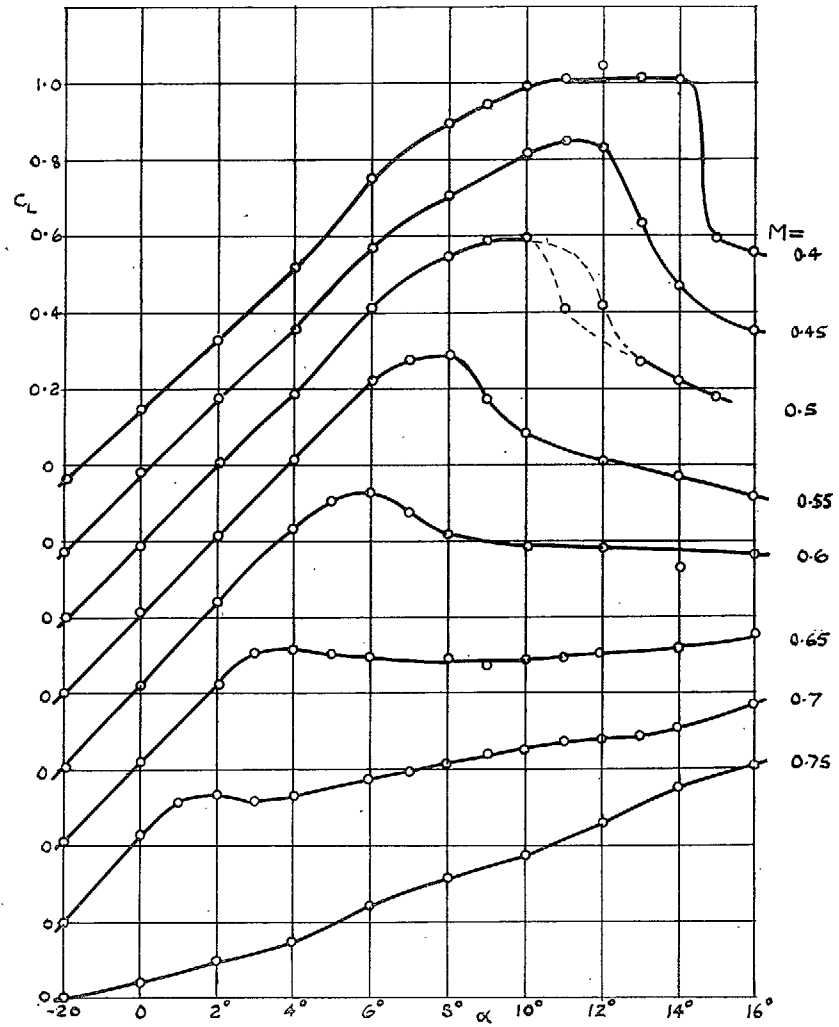

FIG. 2. C_L *vs.* α showing measured points (NACA 2218).

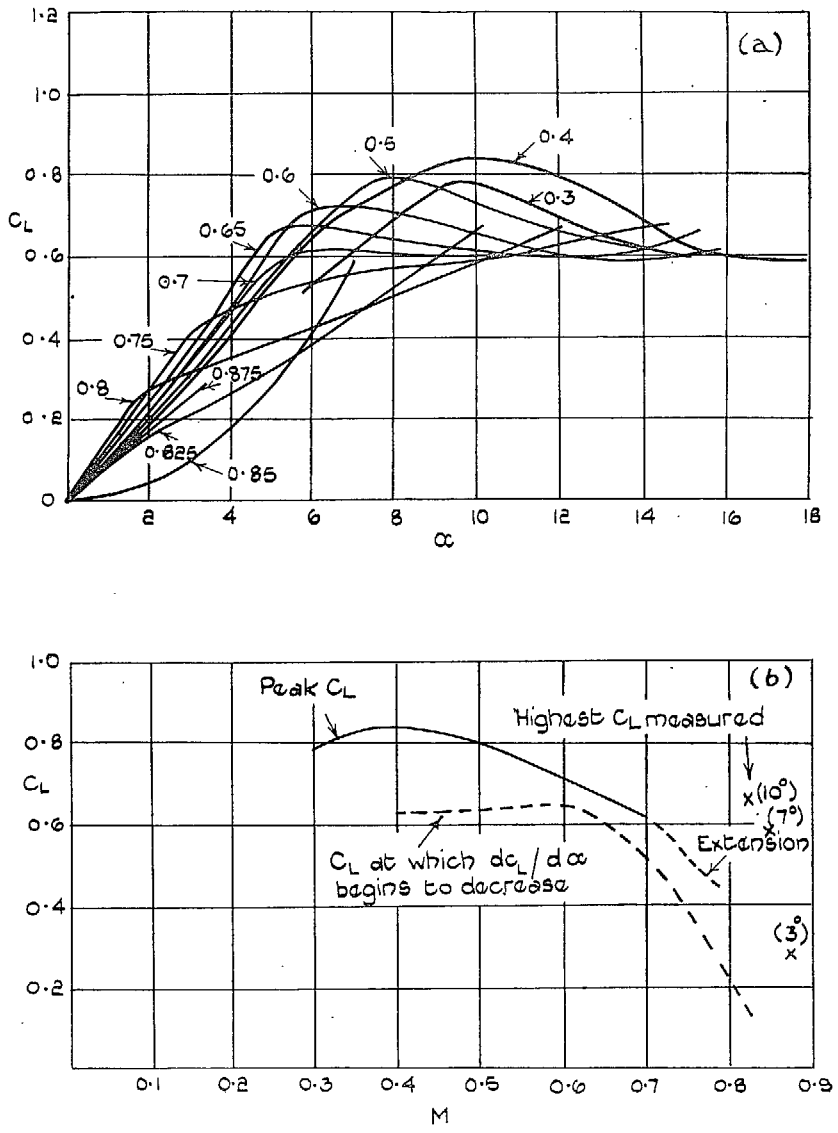

FIG. 3. NACA 0012 (N 1230).

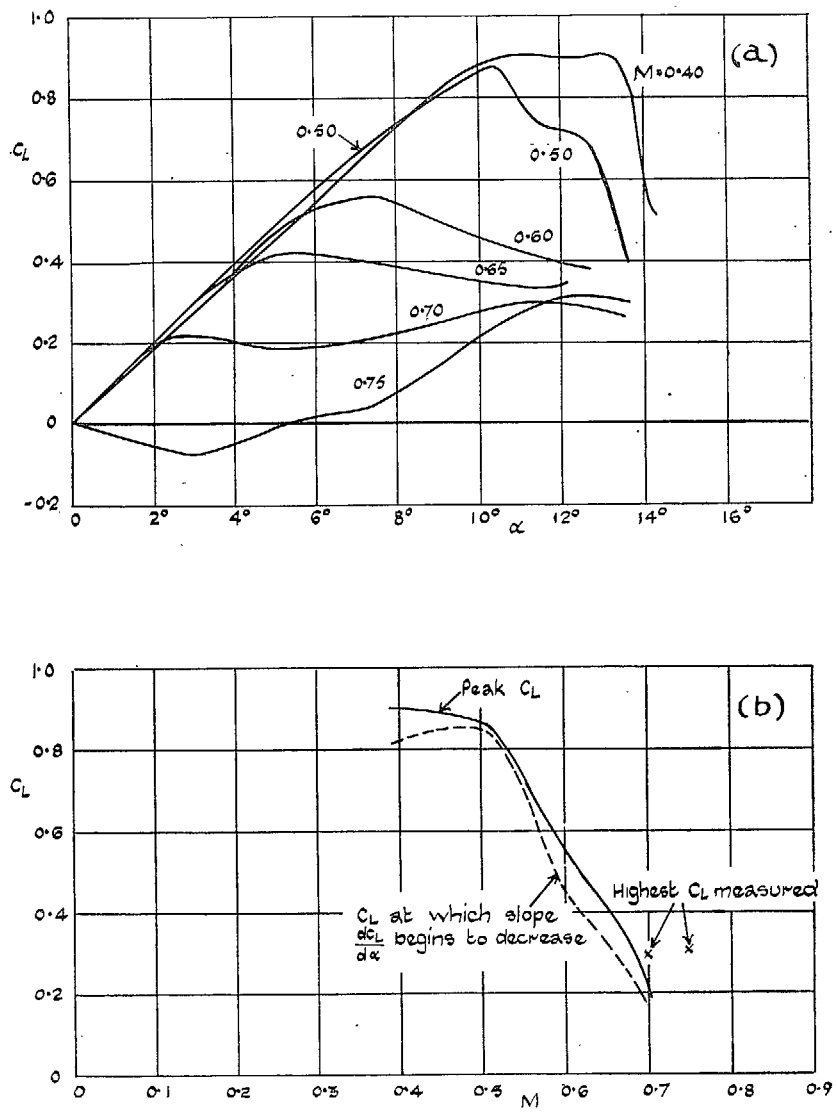

FIG. 4. NACA 0020 (N 2030).

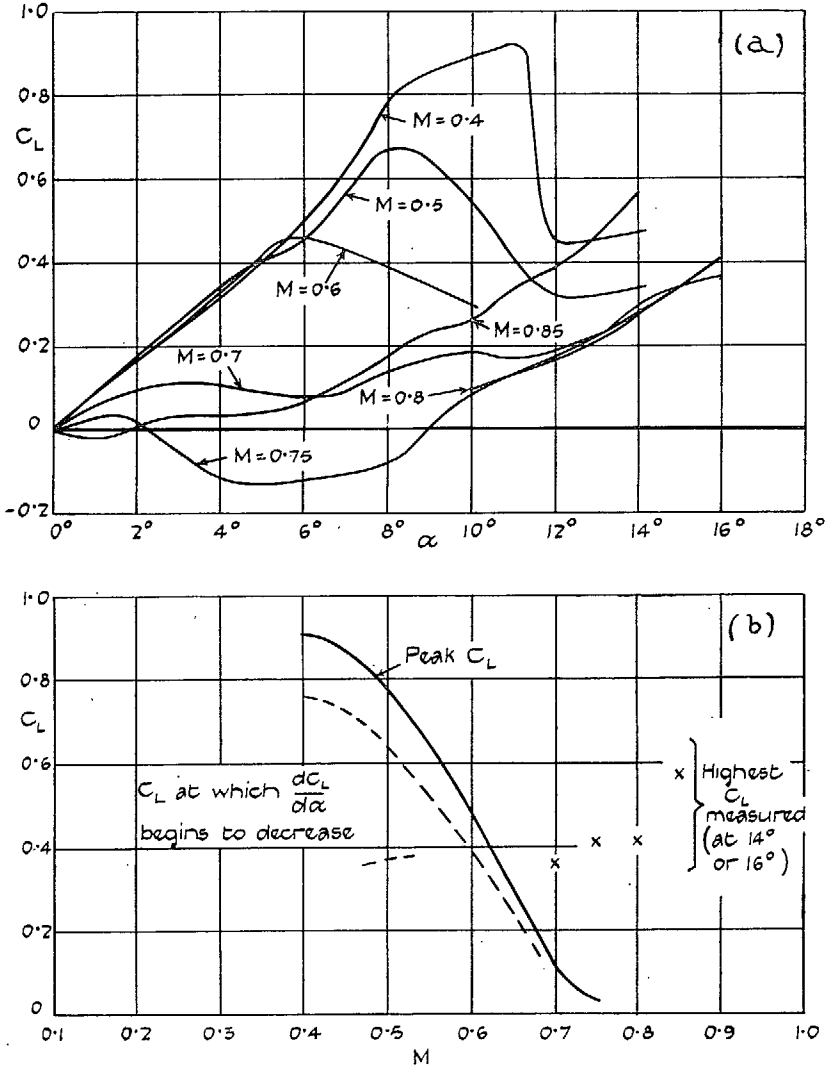

FIG. 5. NACA 0020. 1·2-in. chord.

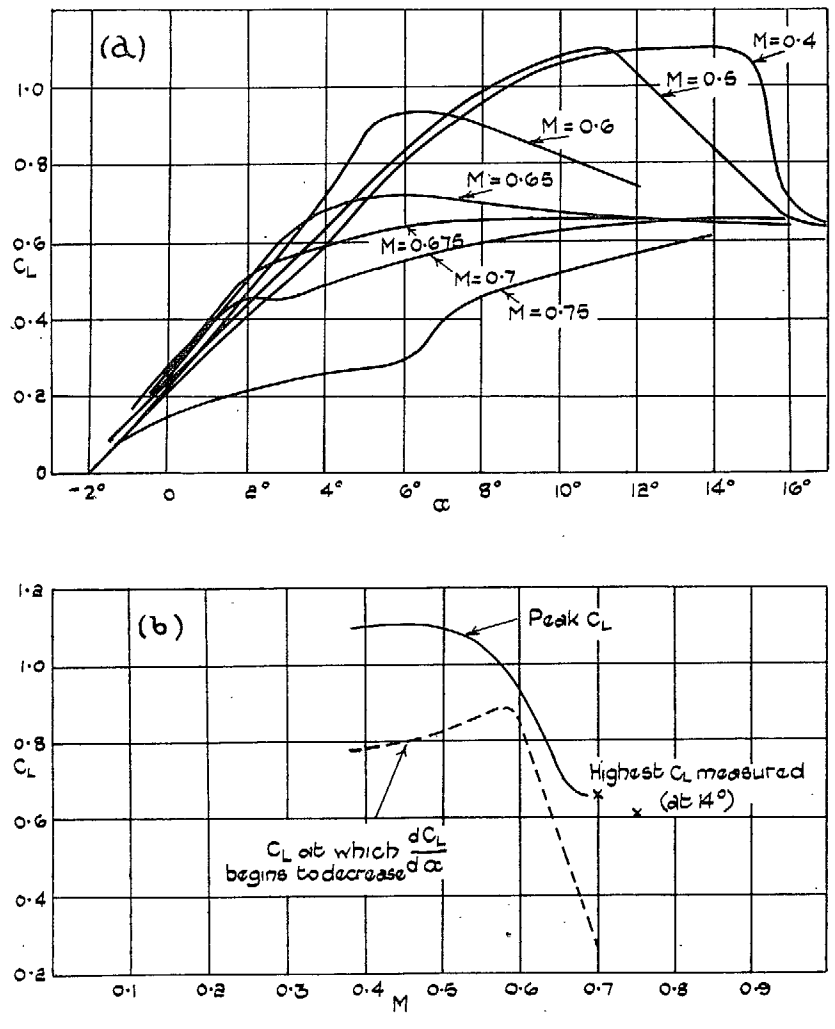

FIG. 6. NACA 2417 (N 1730/2040).

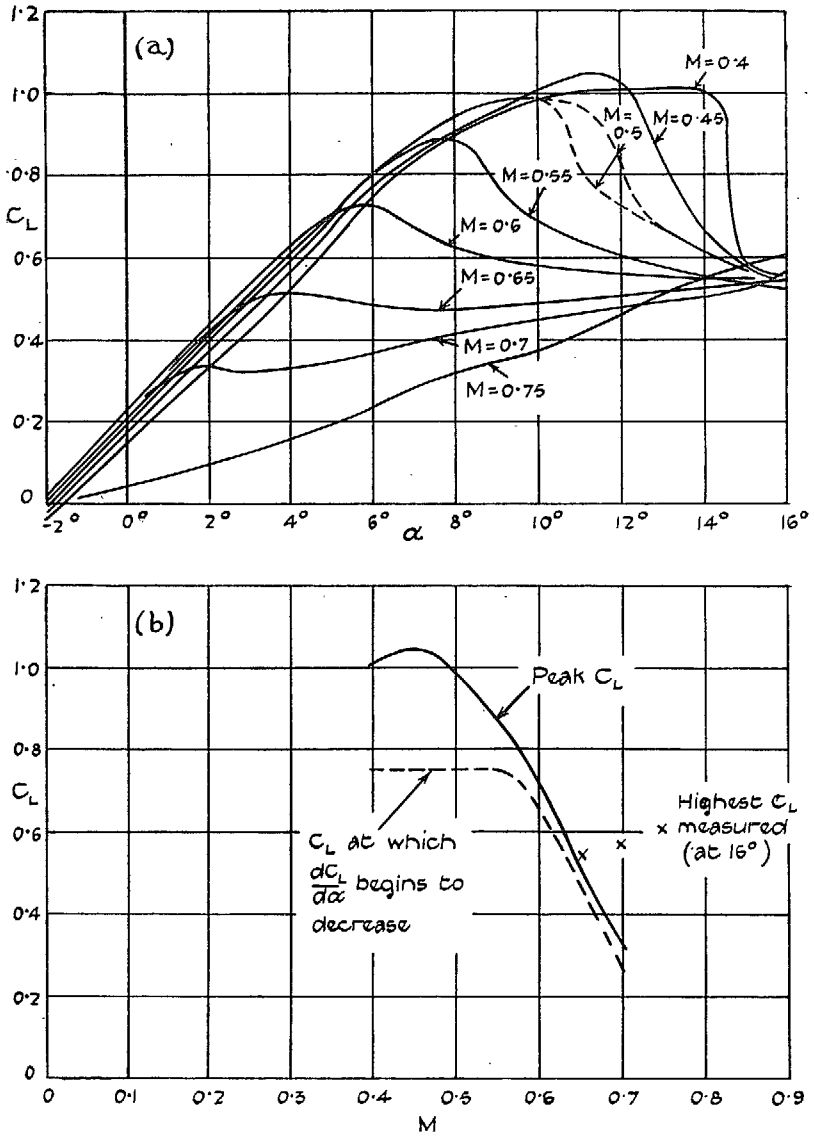

FIG. 7. NACA 2218 (N 1830/2020).

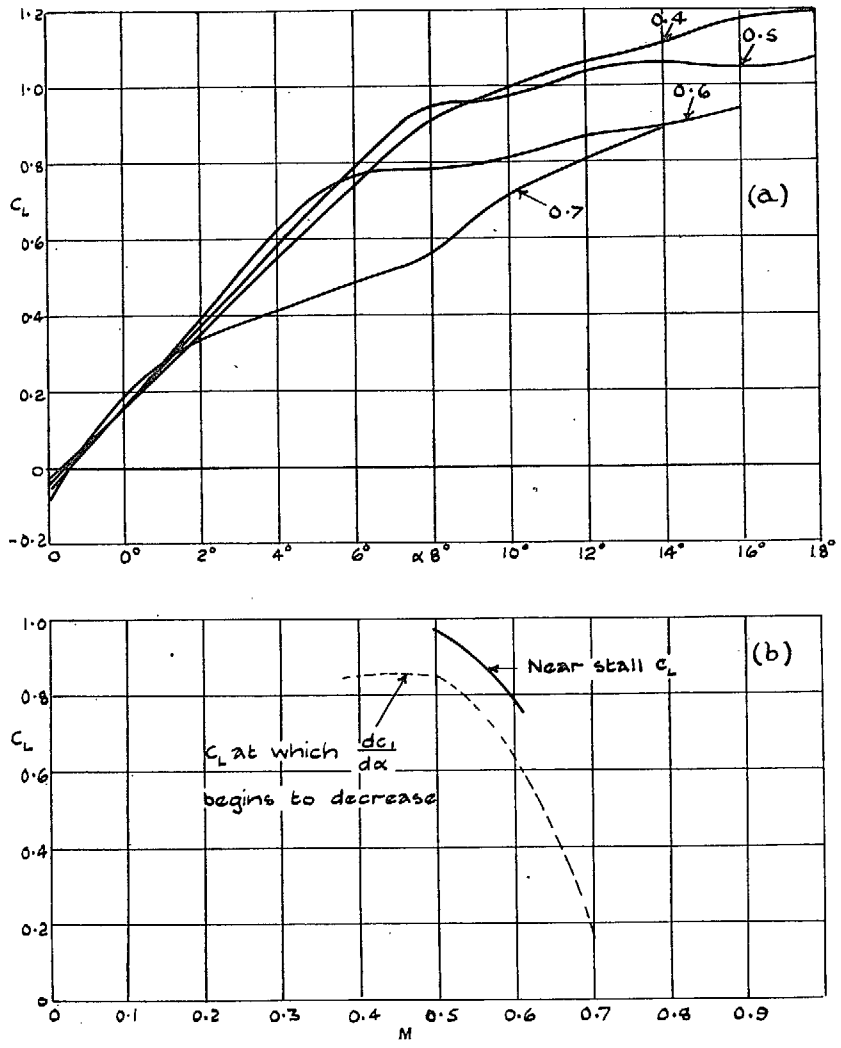

FIG. 8. NACA 2218 5-in. chord.

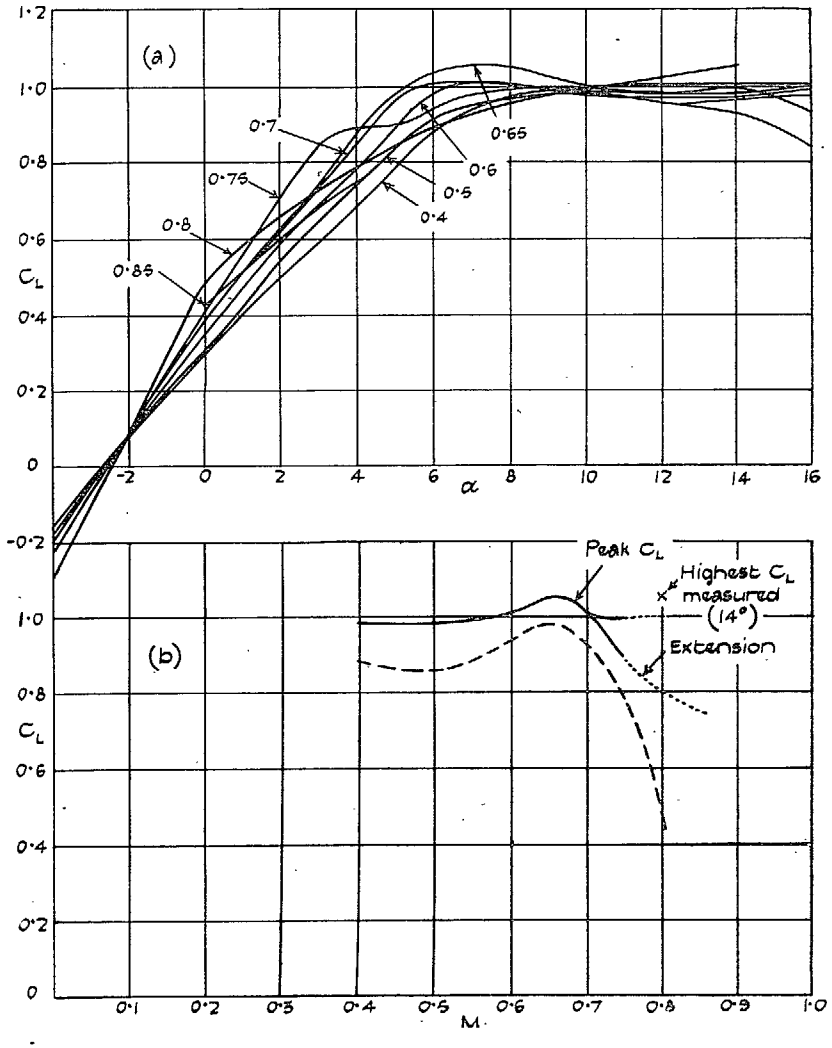

FIG. 9. Clark Y 7 per cent (CY 0733/1741).

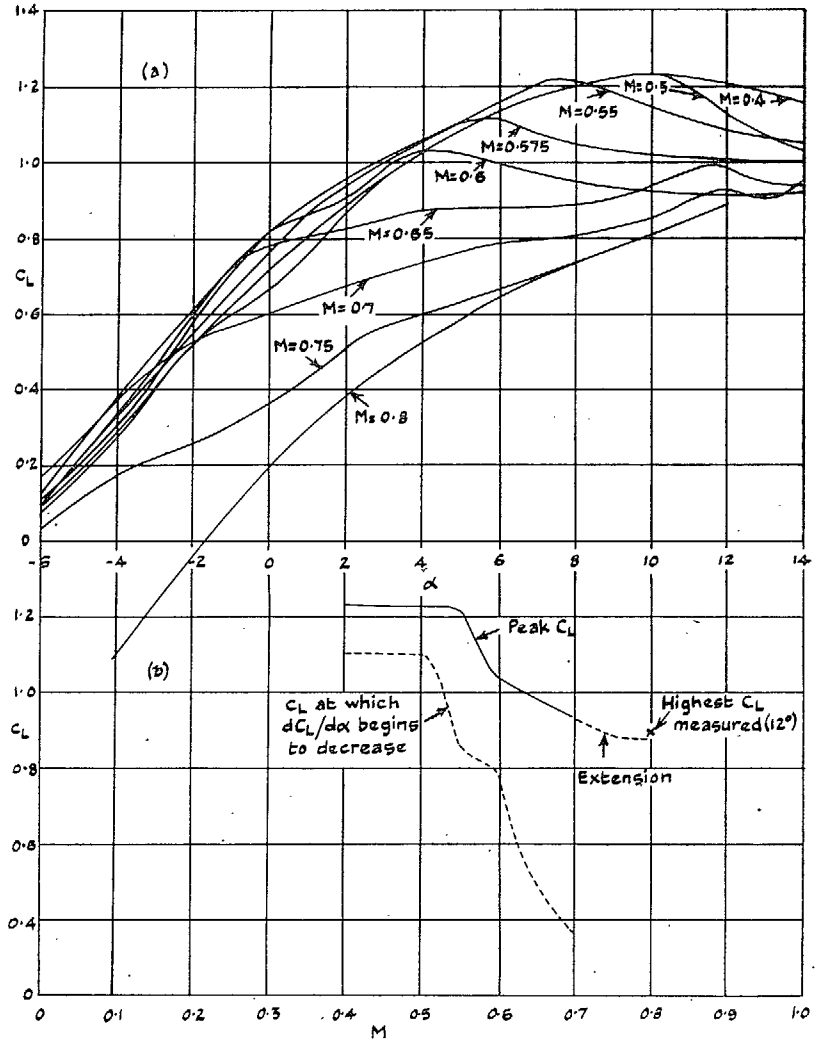

FIG. 10. Clark Y 15 per cent (CY 1533/4341).

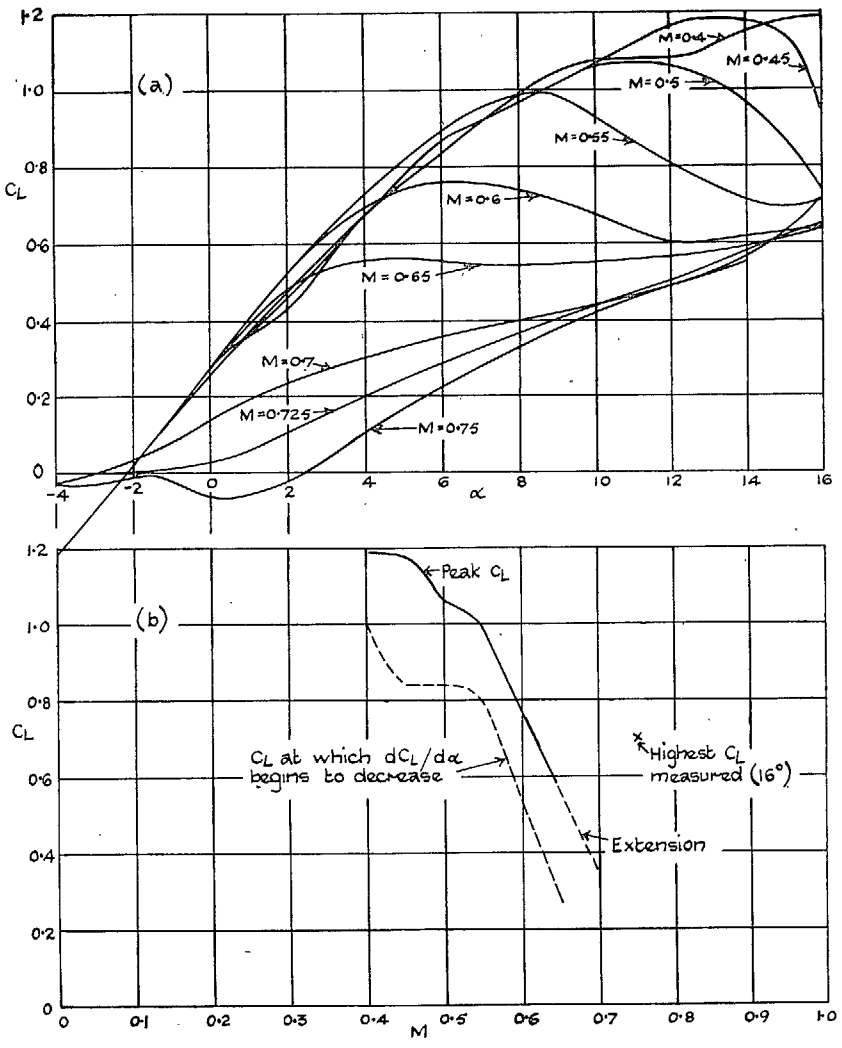

FIG. 11. RAF 69. R 2131/1944.

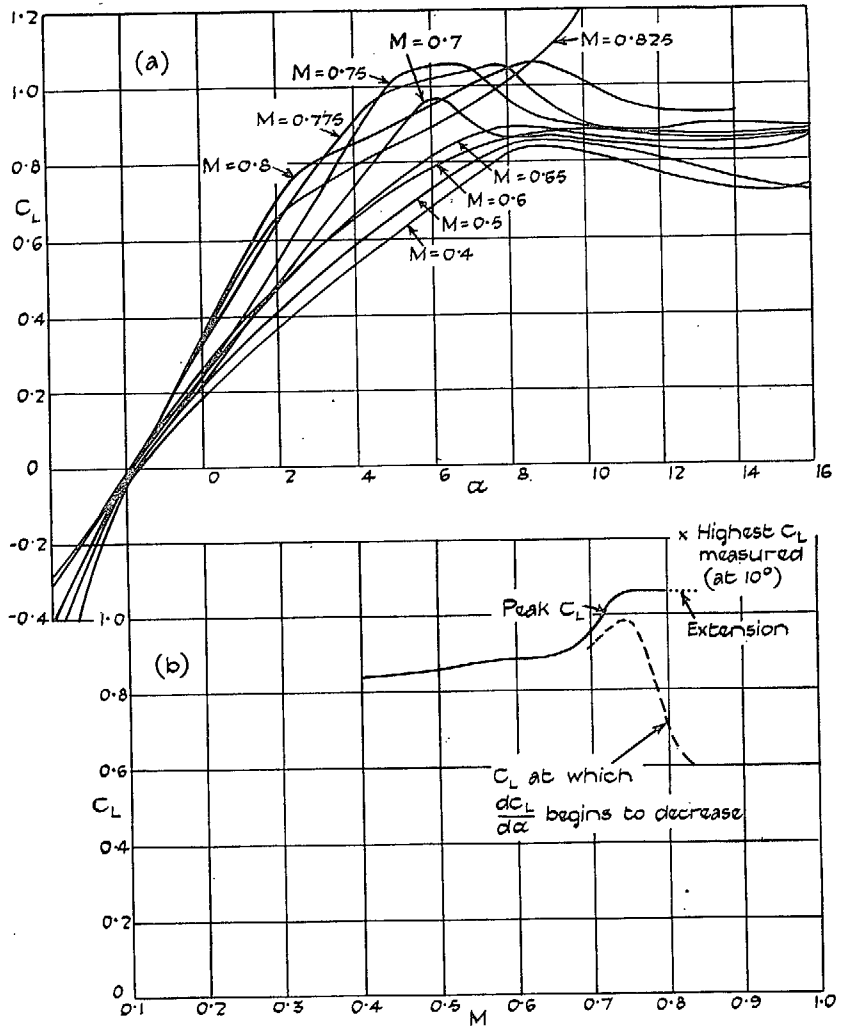

FIG. 12. NACA 1615 (NL 0650/1250).

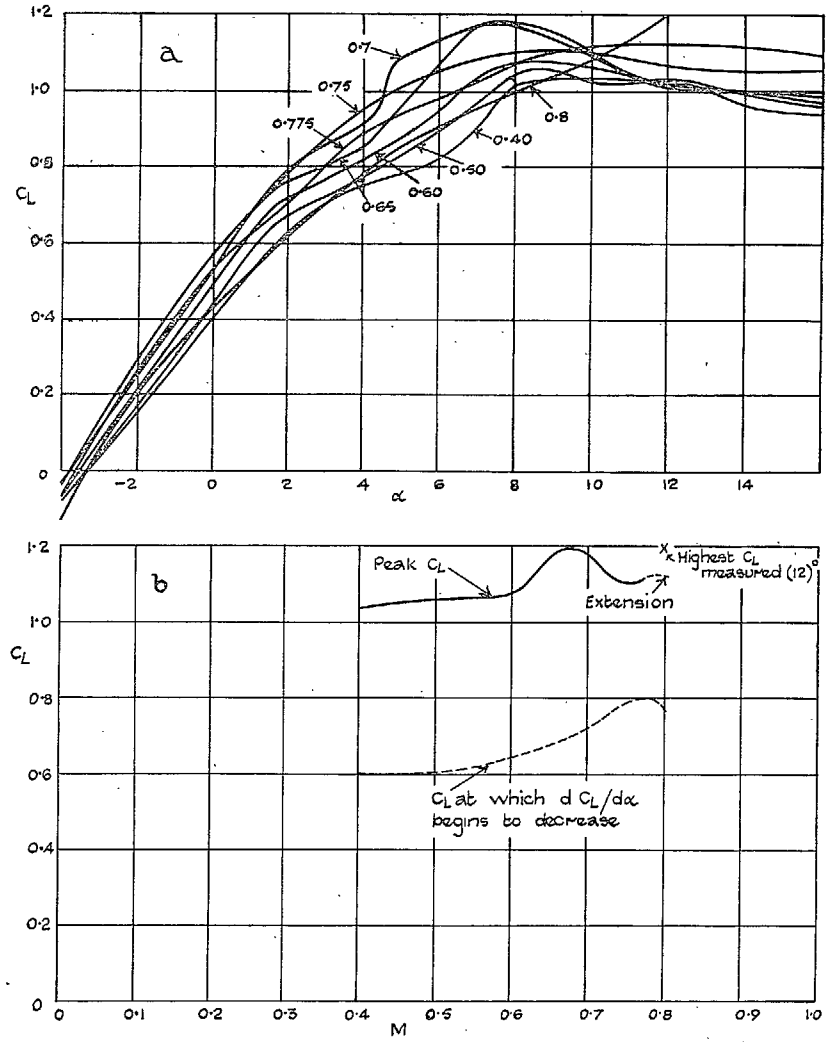

FIG. 13. NACA 1621 (NL 0750/3050).

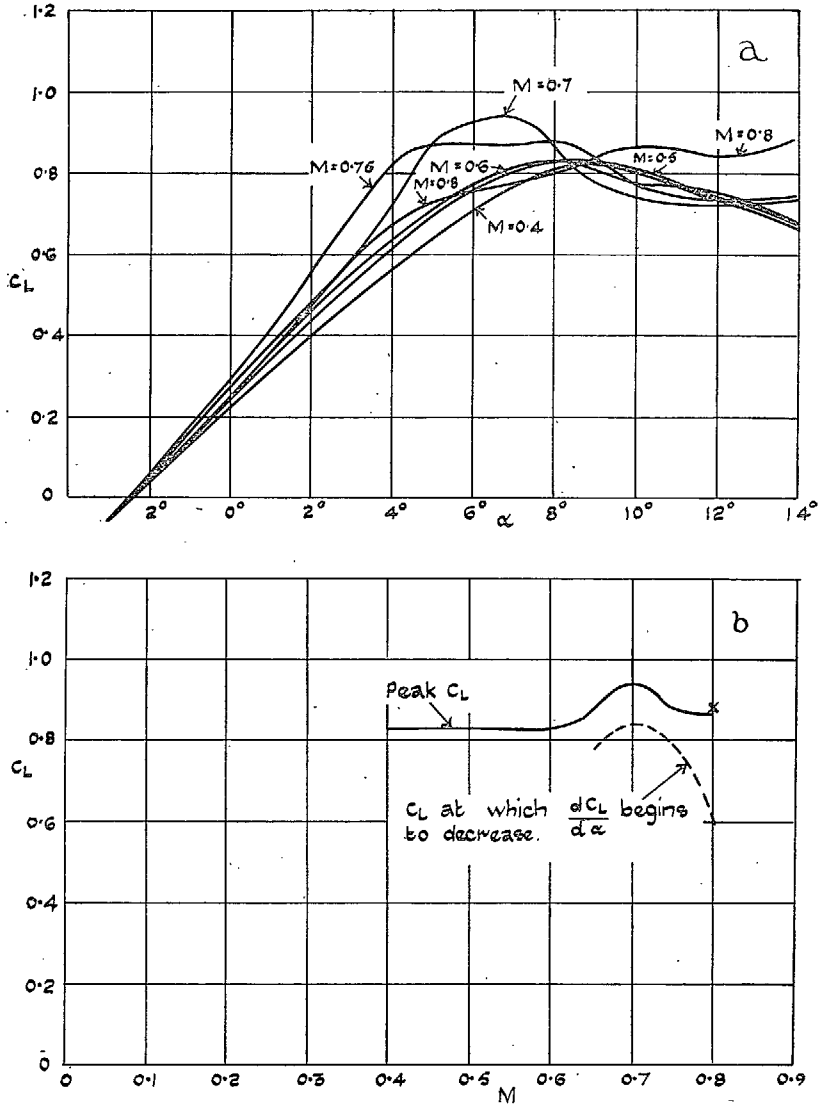

FIG. 14. NACA 16/12 (NL 1050/1250).

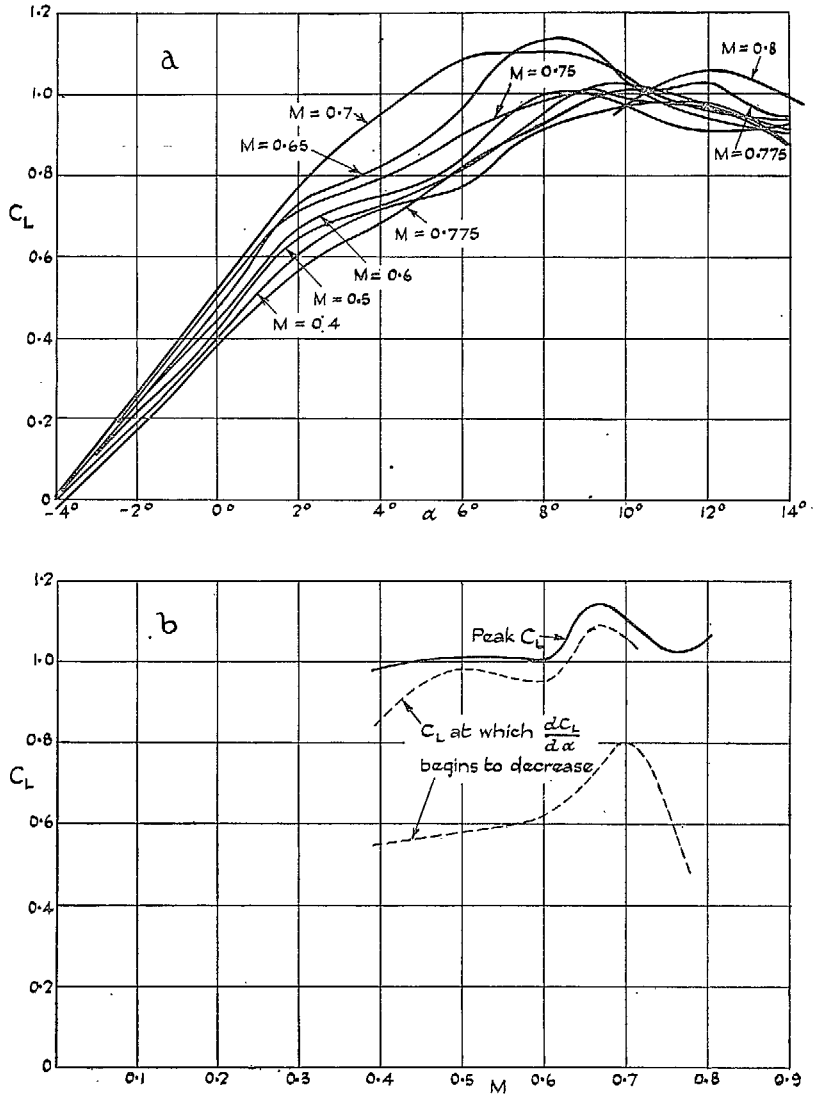

FIG. 15. NACA 16/22 (NL 1050/3050).

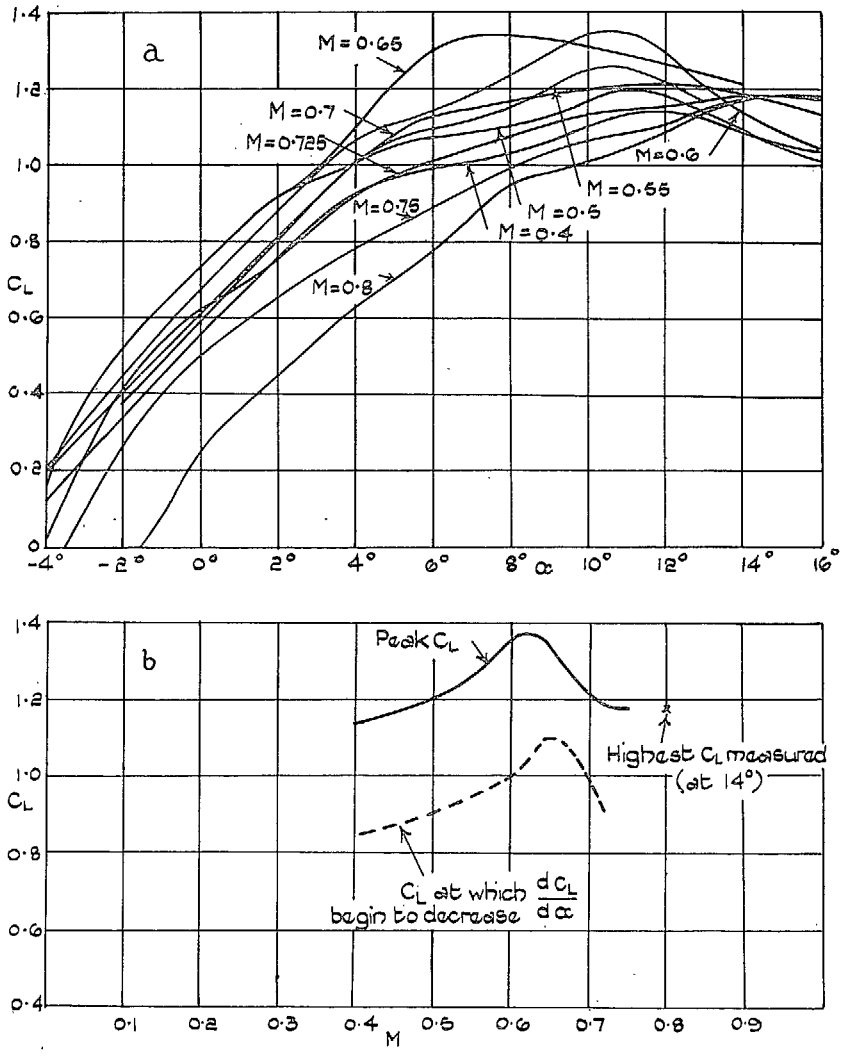

FIG. 16. NACA 16/32 (NL 1050/4850).

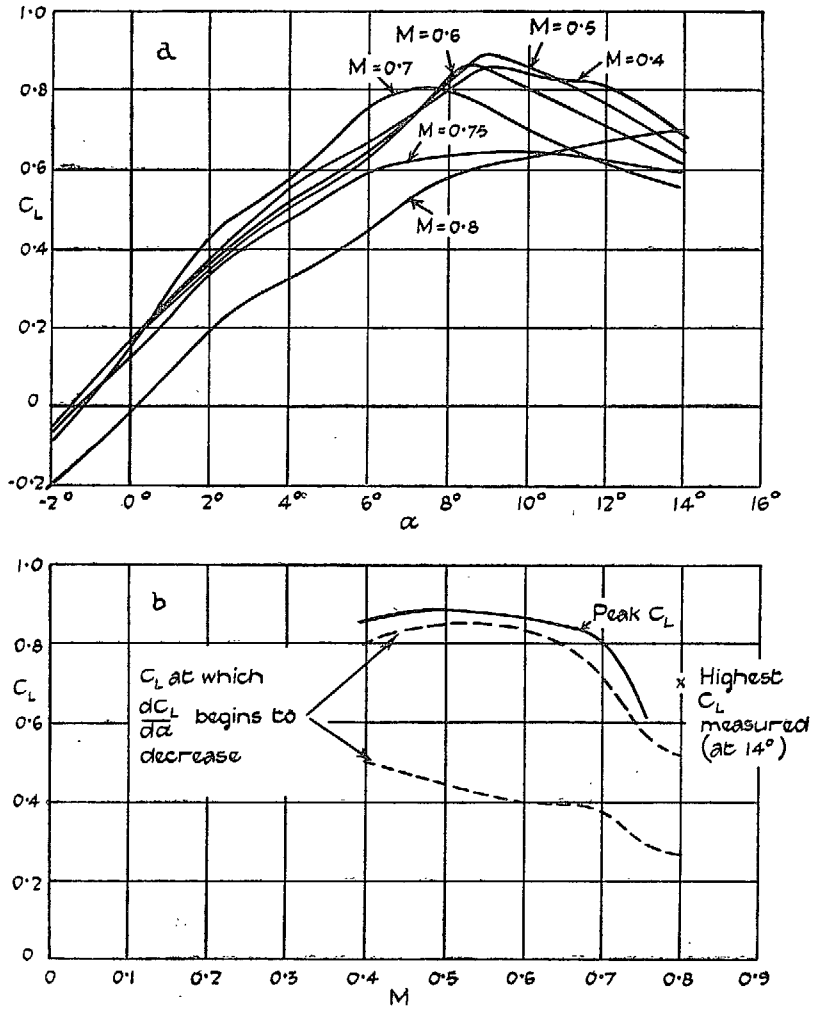

FIG. 17. NACA 1616 (NL 1550/1250).

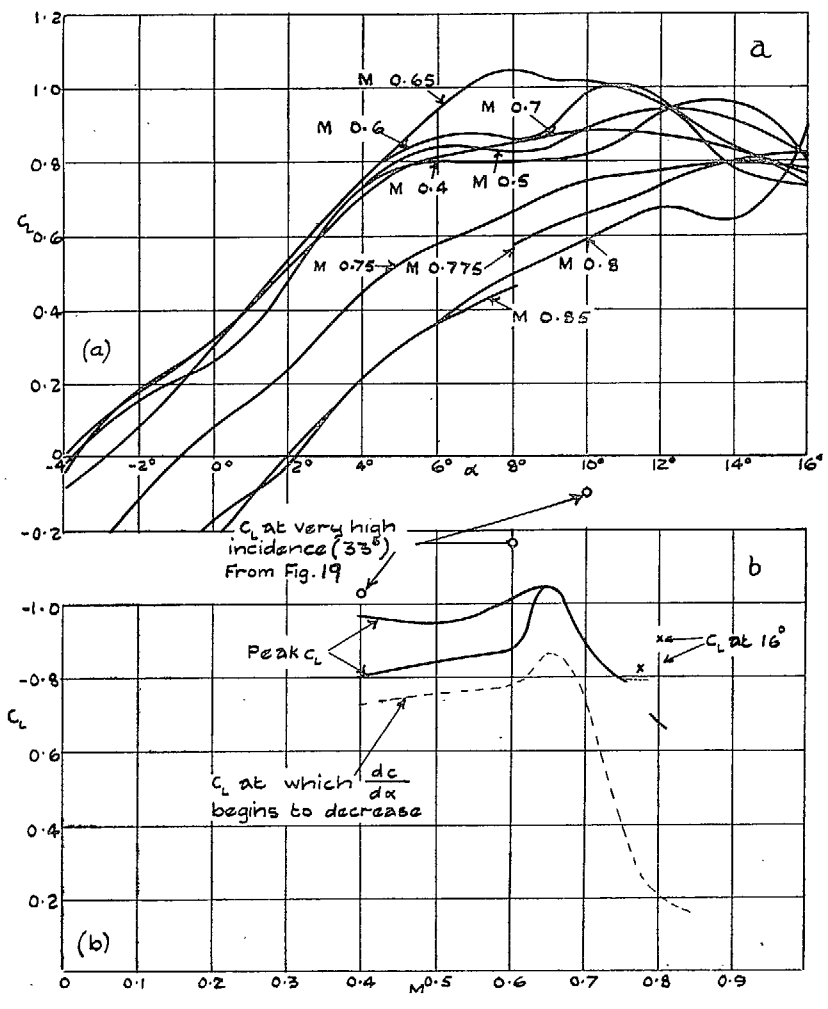

FIG. 18. NACA 16/26 (NL 1550/3050).

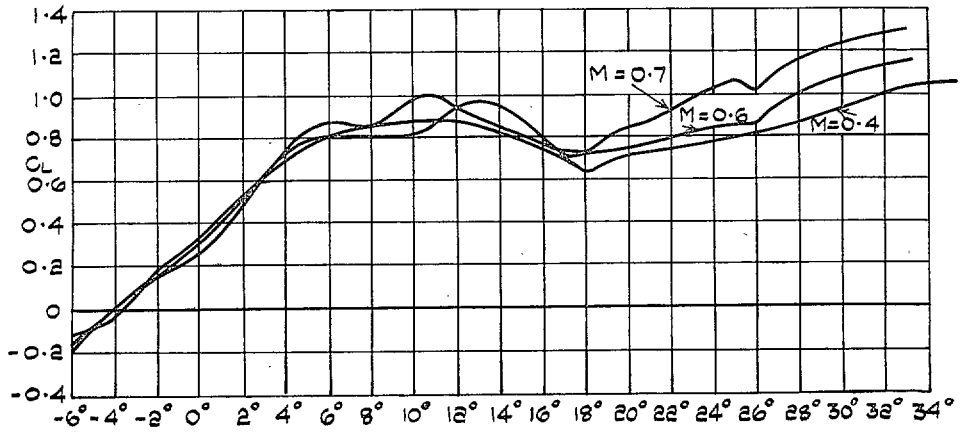

FIG. 19. NACA 16/26 (NL 1550/3050). Large angles of incidence.

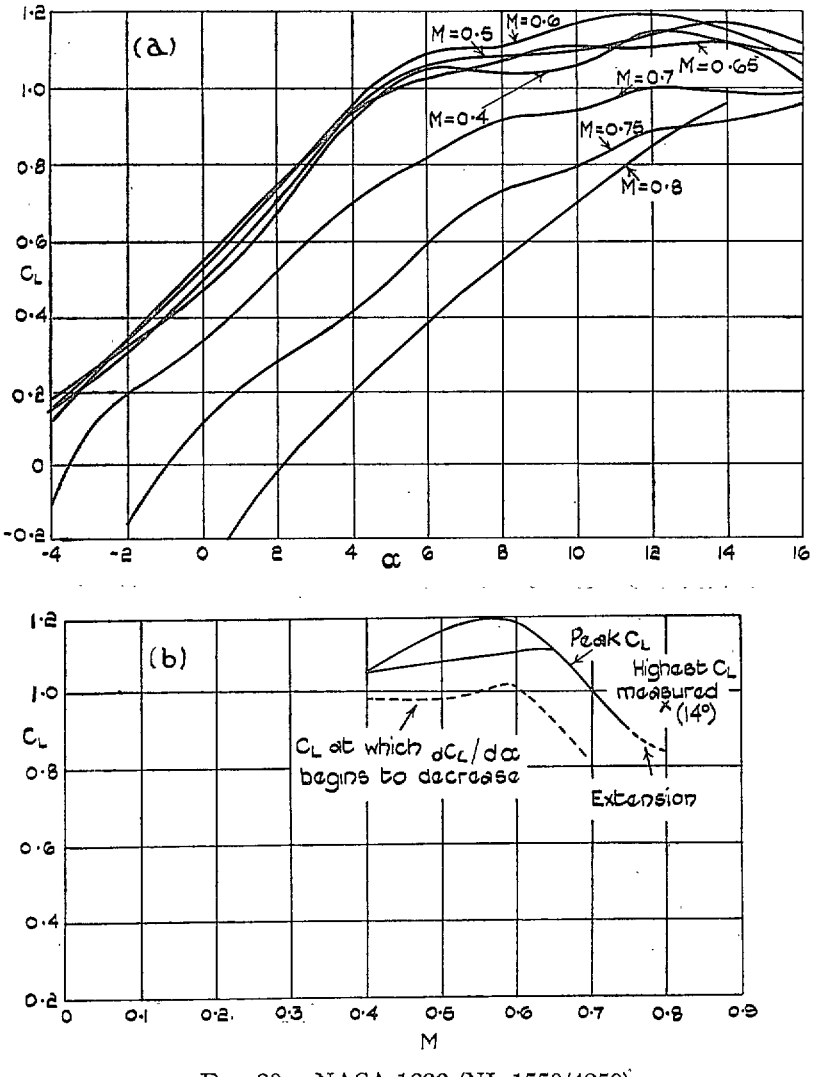

FIG. 20. NACA 1636 (NL 1550/4850).

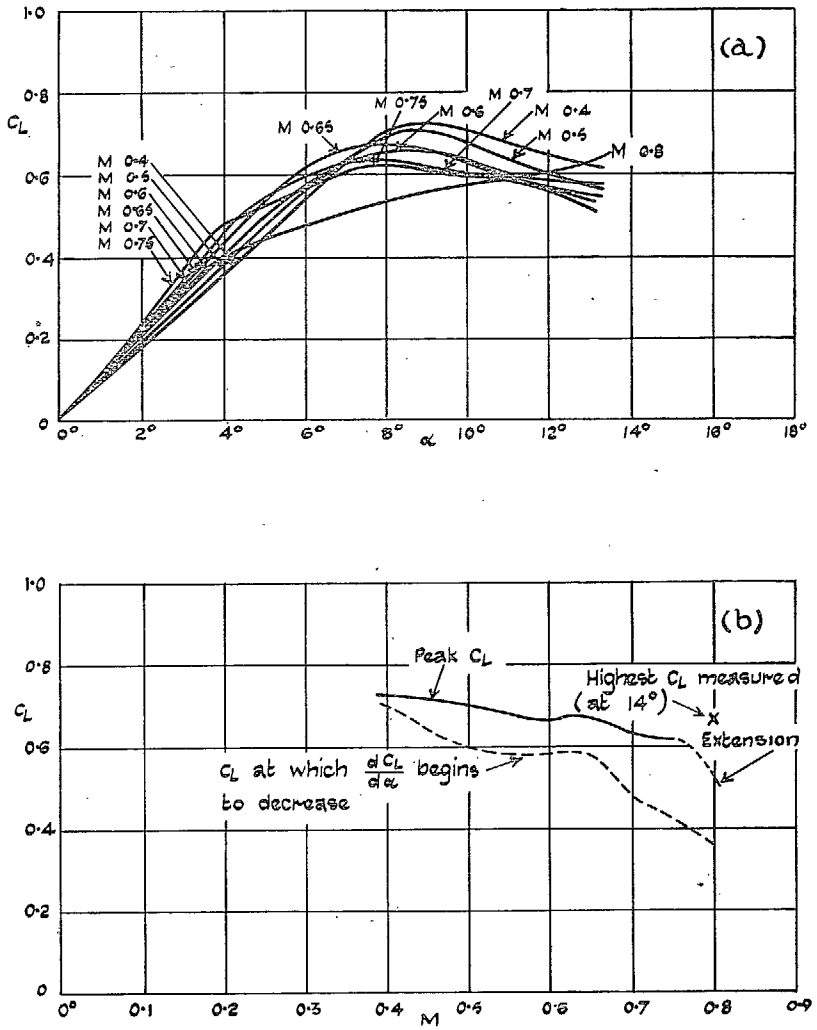

FIG. 21. EC 1240.

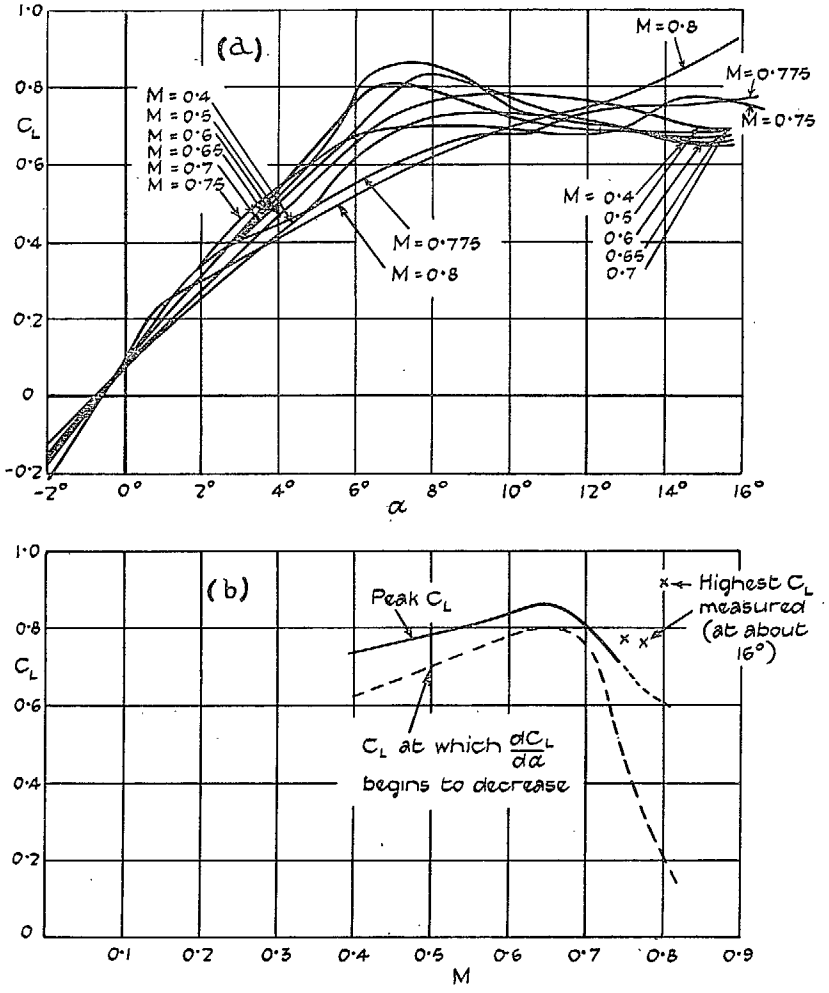

FIG. 22. EC 1240/0640.

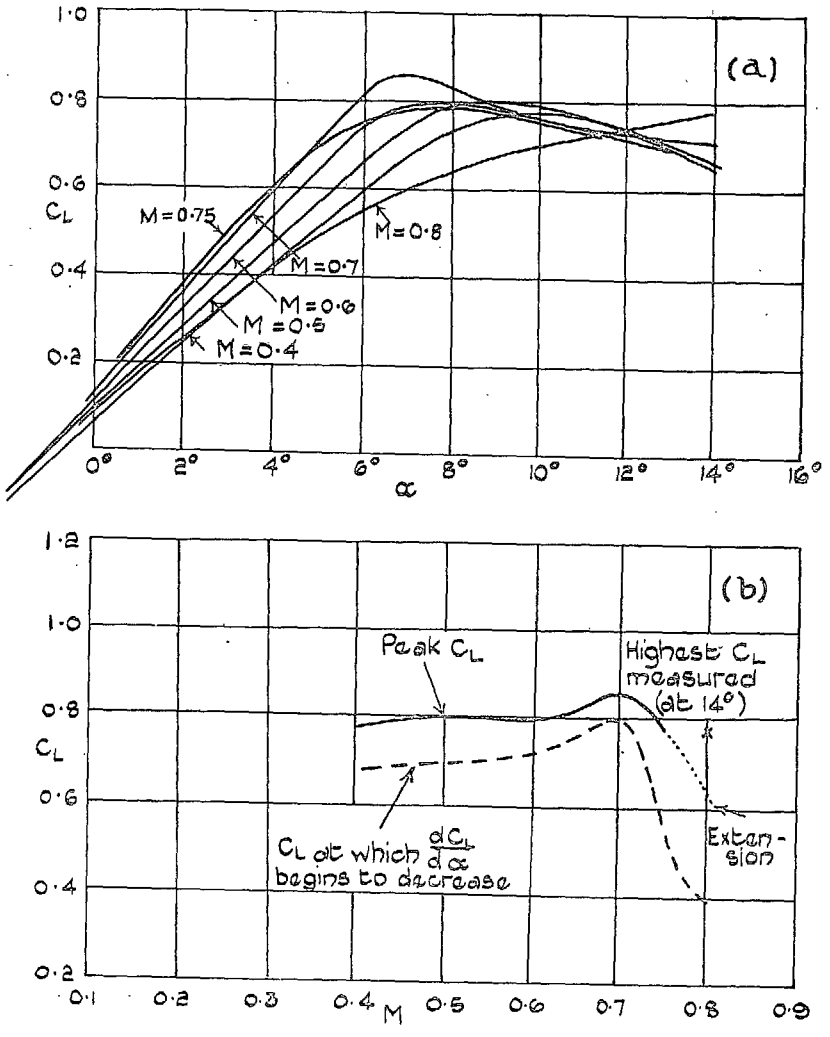

FIG. 23. EC 1240/0658.

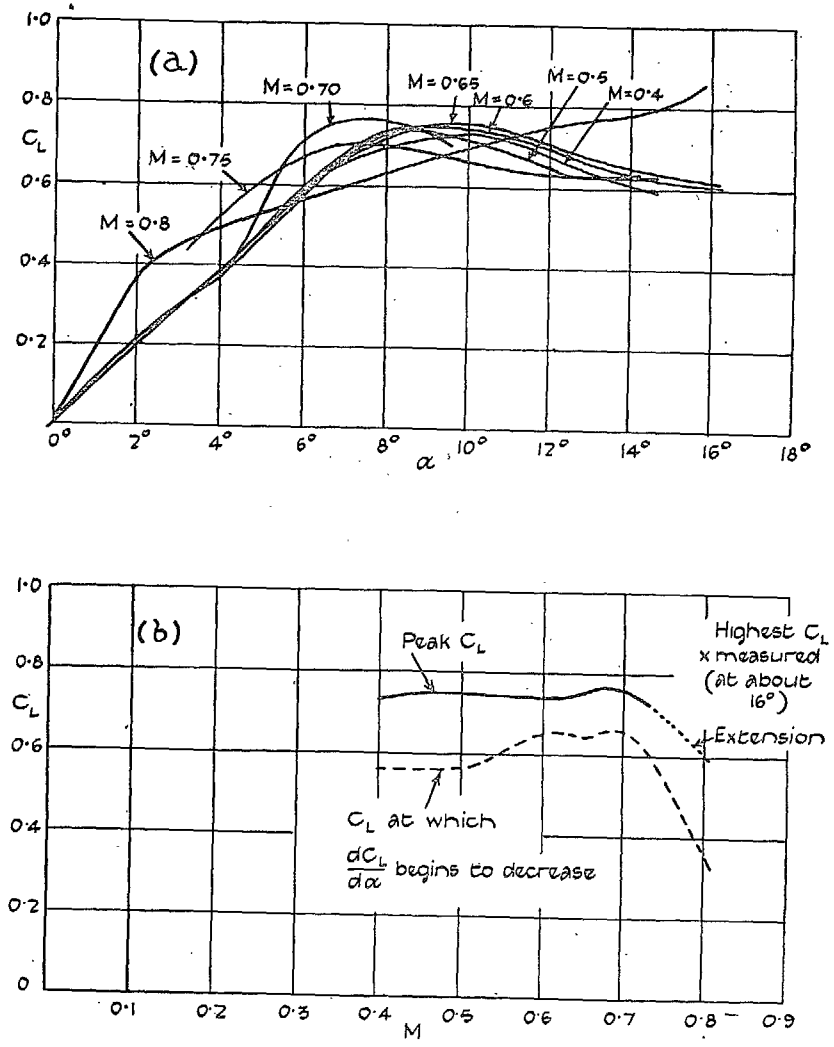

FIG. 24. EC 1250.

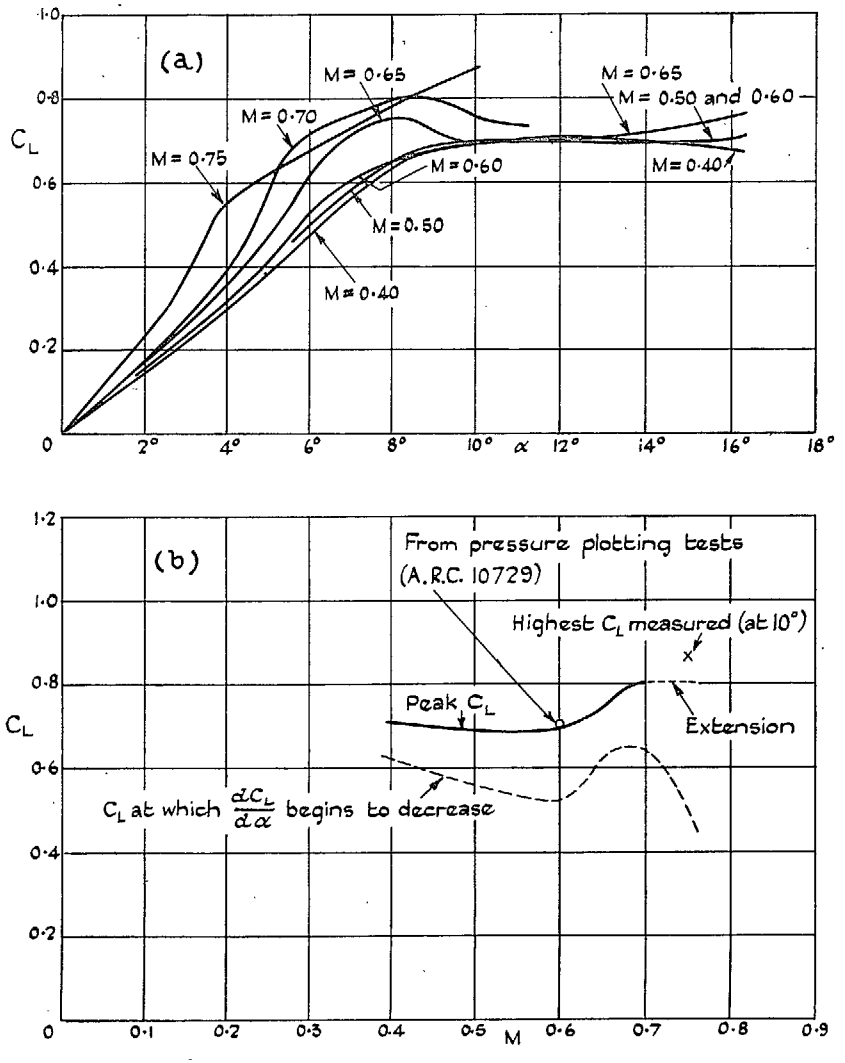

FIG. 25. EC 1250 5-in. chord (uncorrected for straight walls).

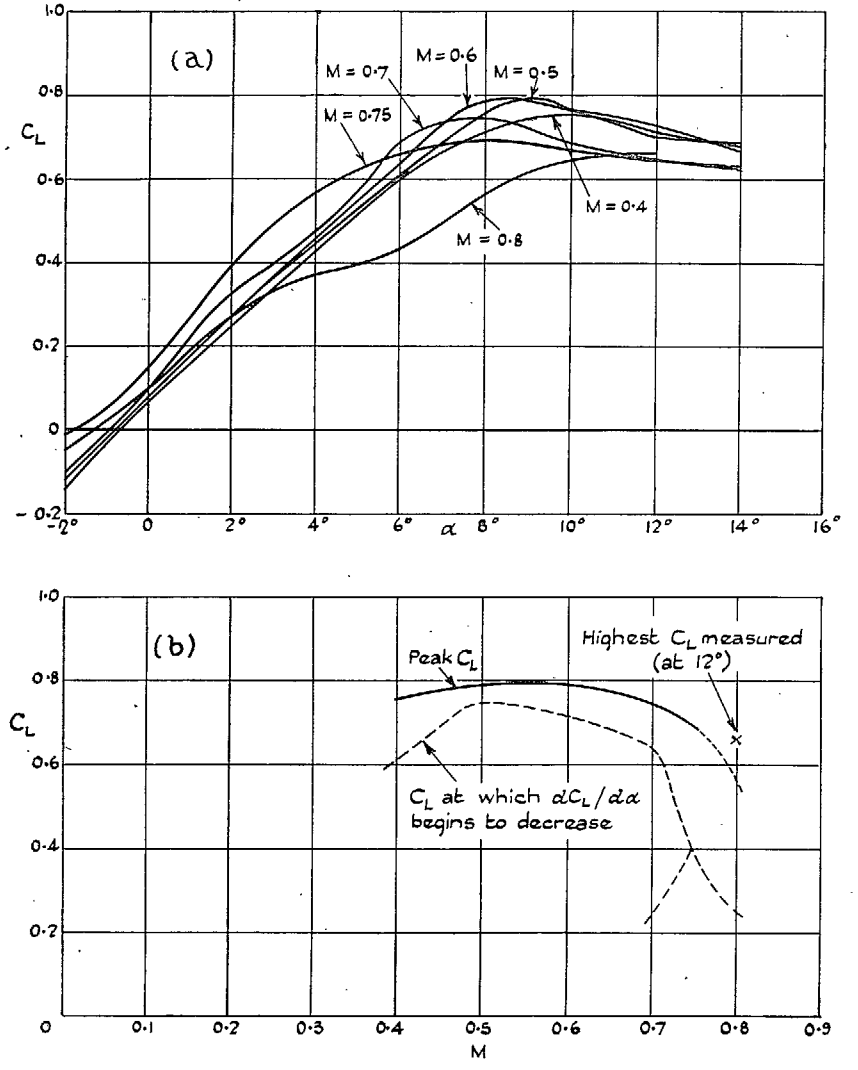

FIG. 26. EQH 1250/0640.

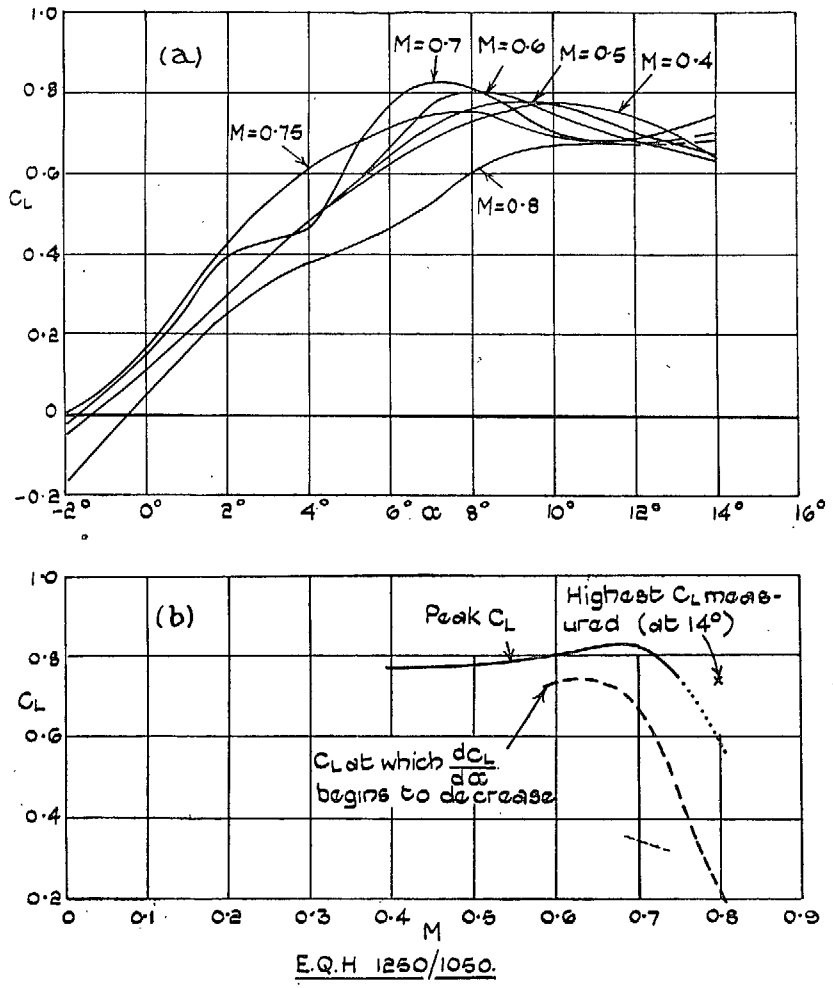

FIG. 27. EQH 1250/1050.

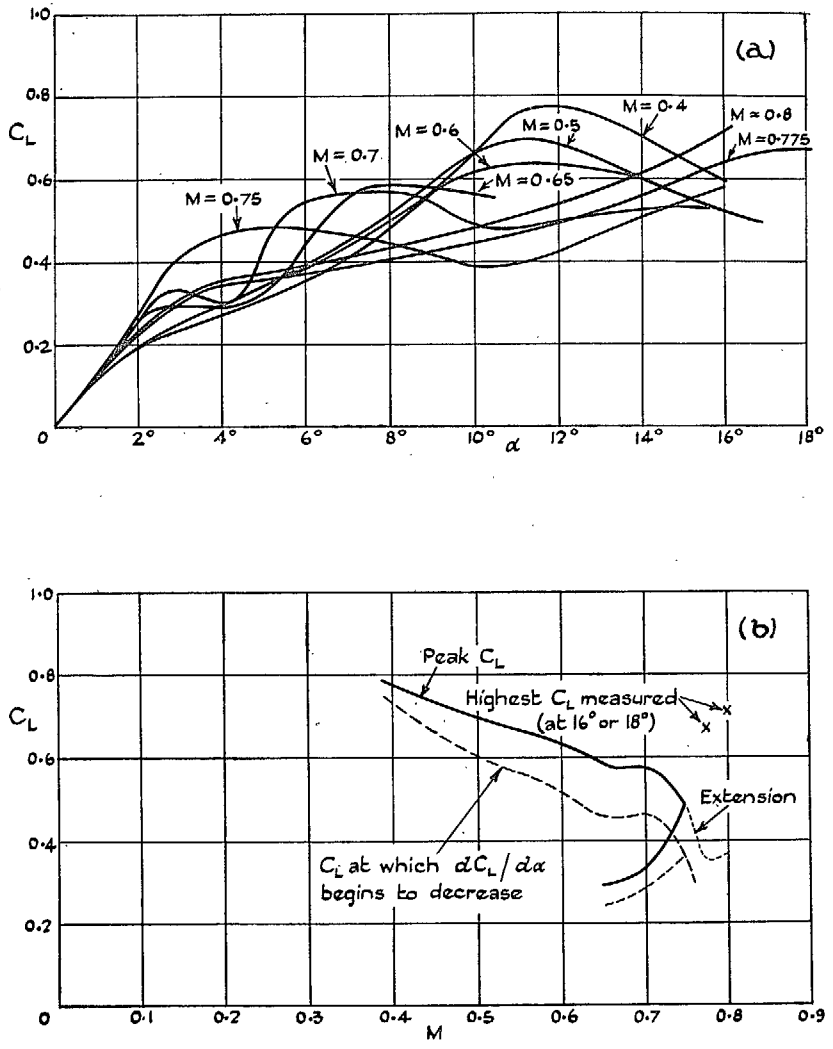

FIG. 28. EQH 1550.

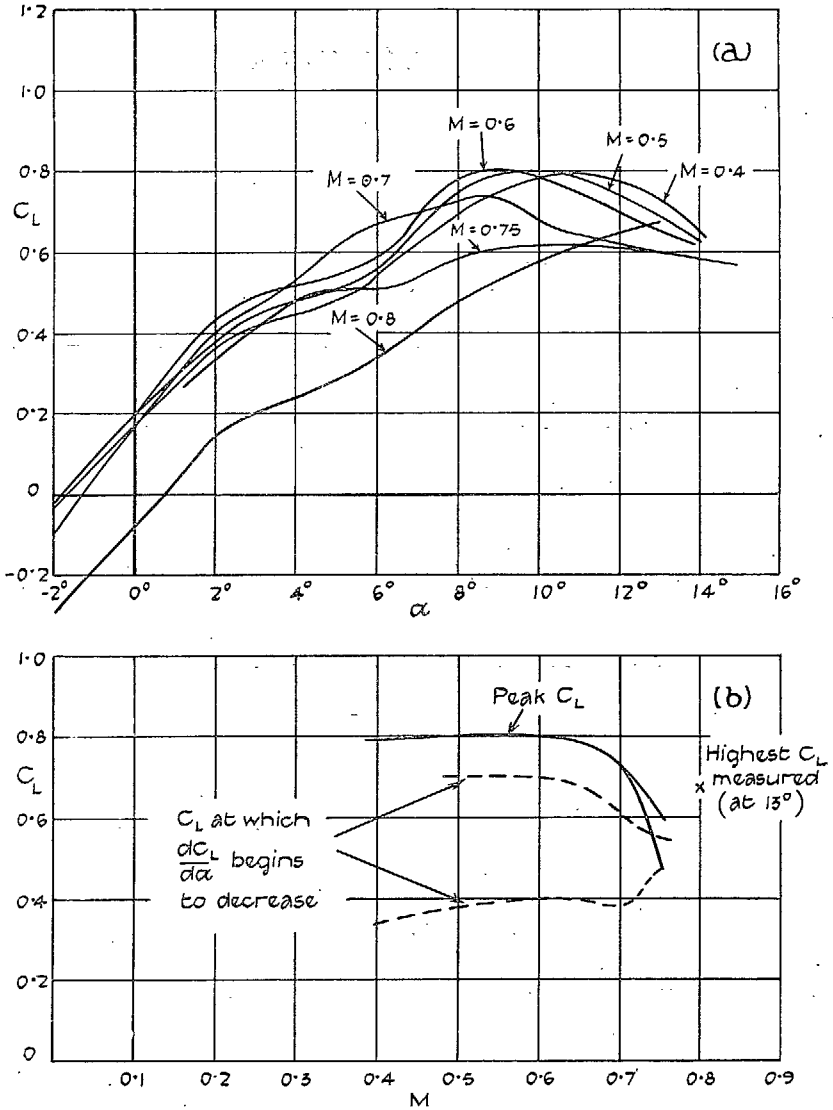

FIG. 29. EQH 1550/1058.

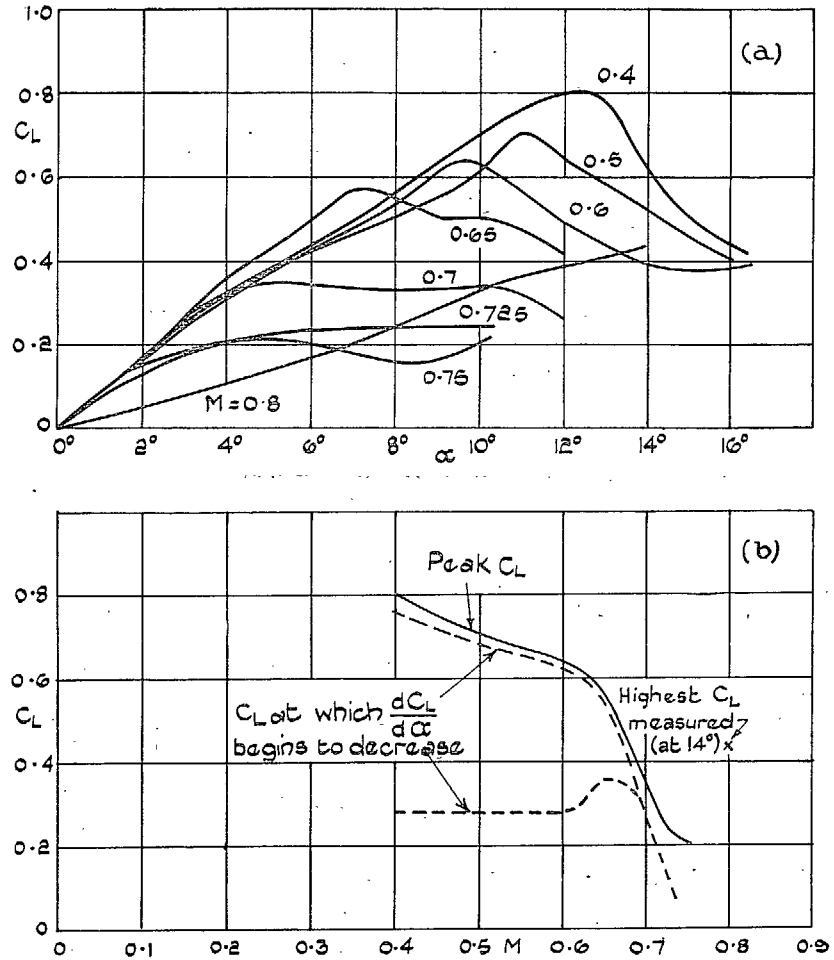

FIG. 30. Piercy 2040.

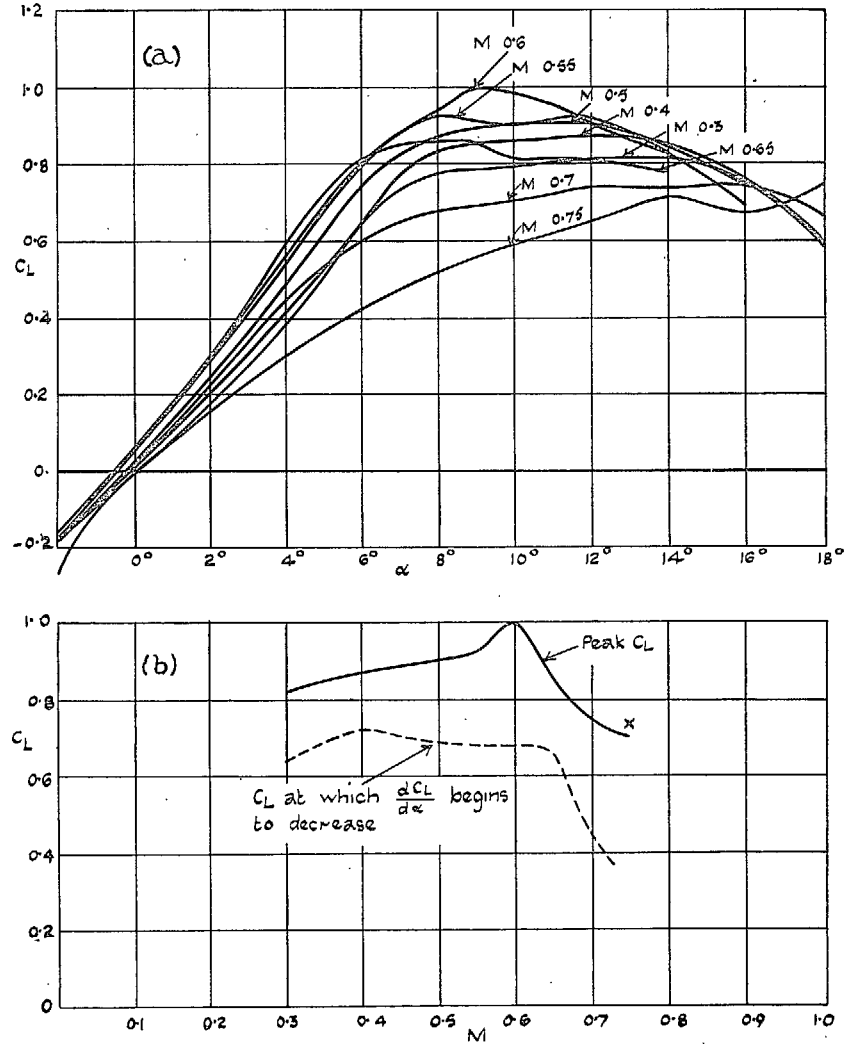

FIG. 31. Goldstein-Richards reflex 1540/2037.

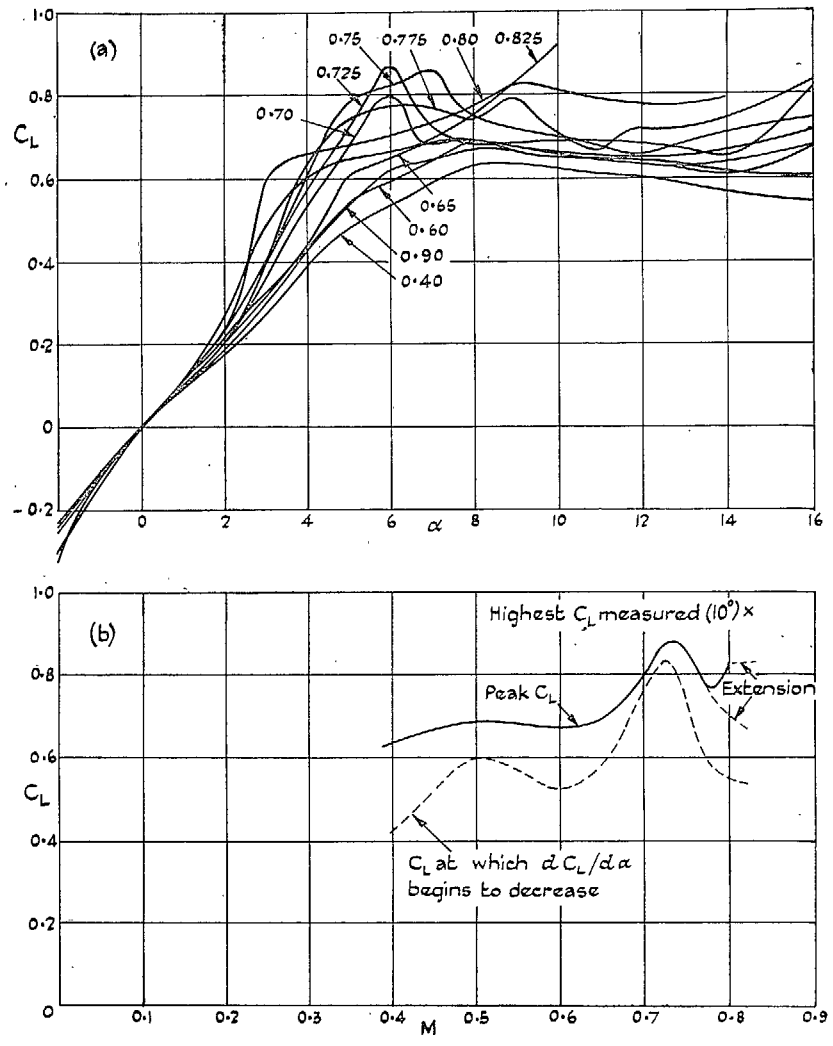

FIG. 32. Biconvex 07½50.

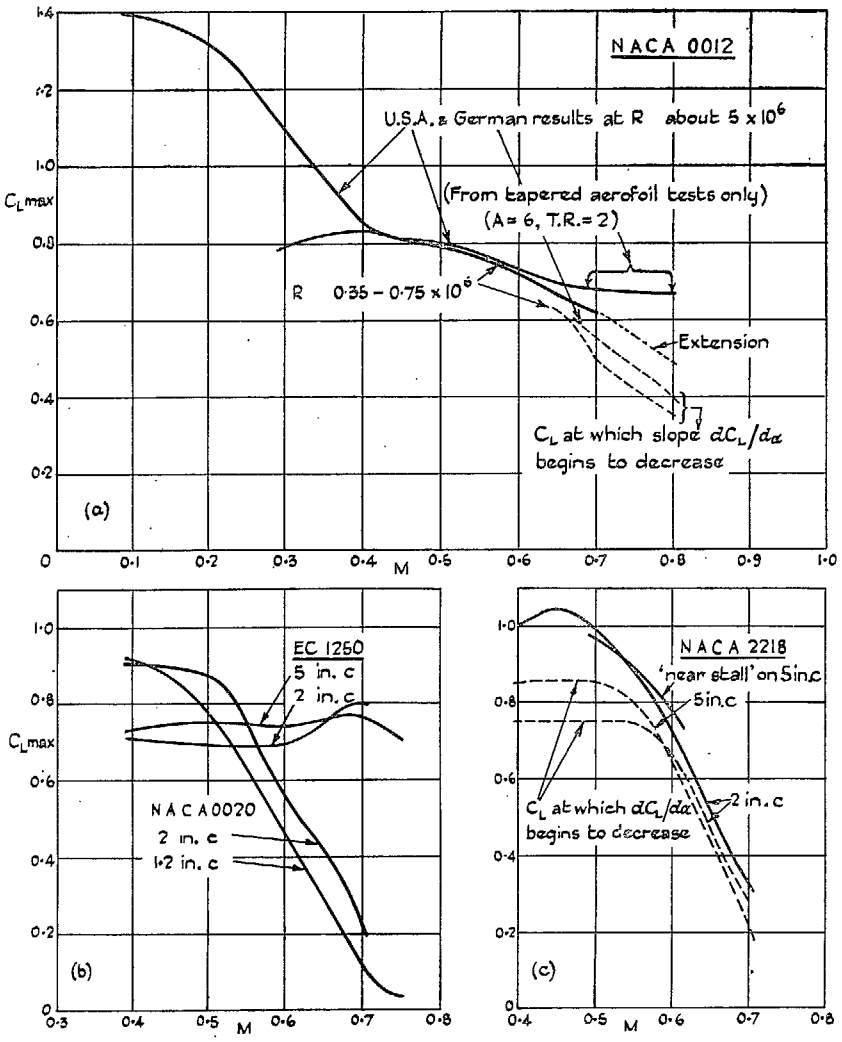

FIG. 33. Effect of Reynolds number.

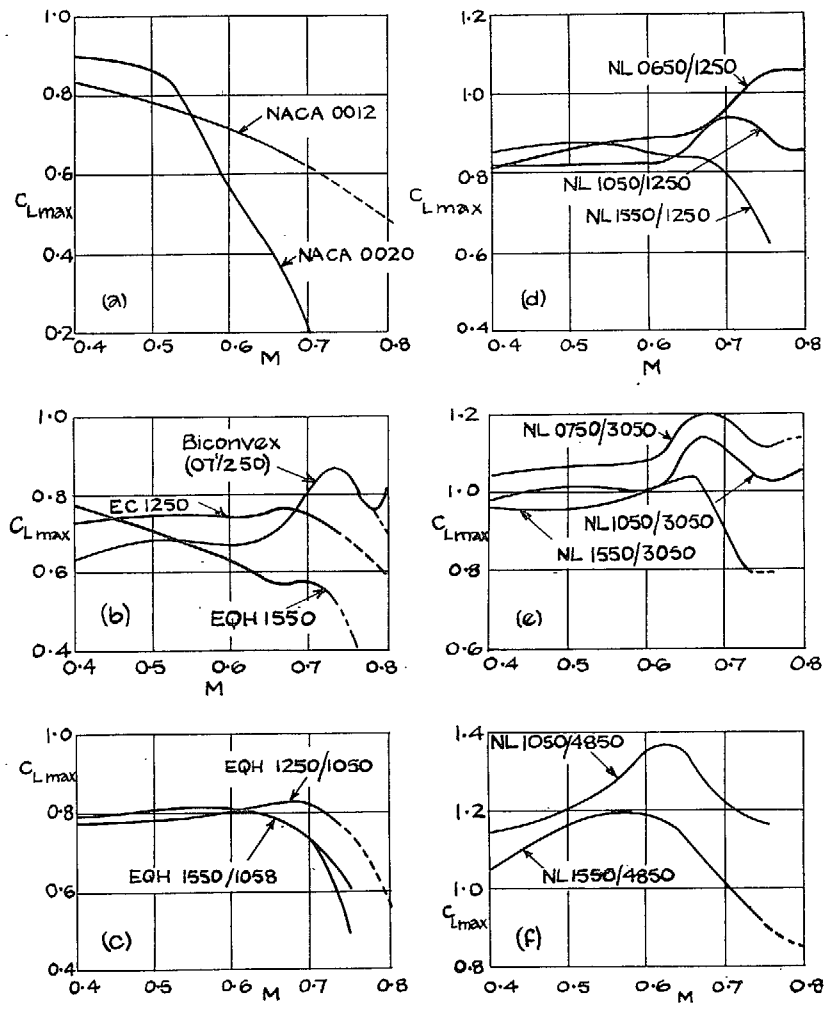

FIG. 34. Effect of thickness.

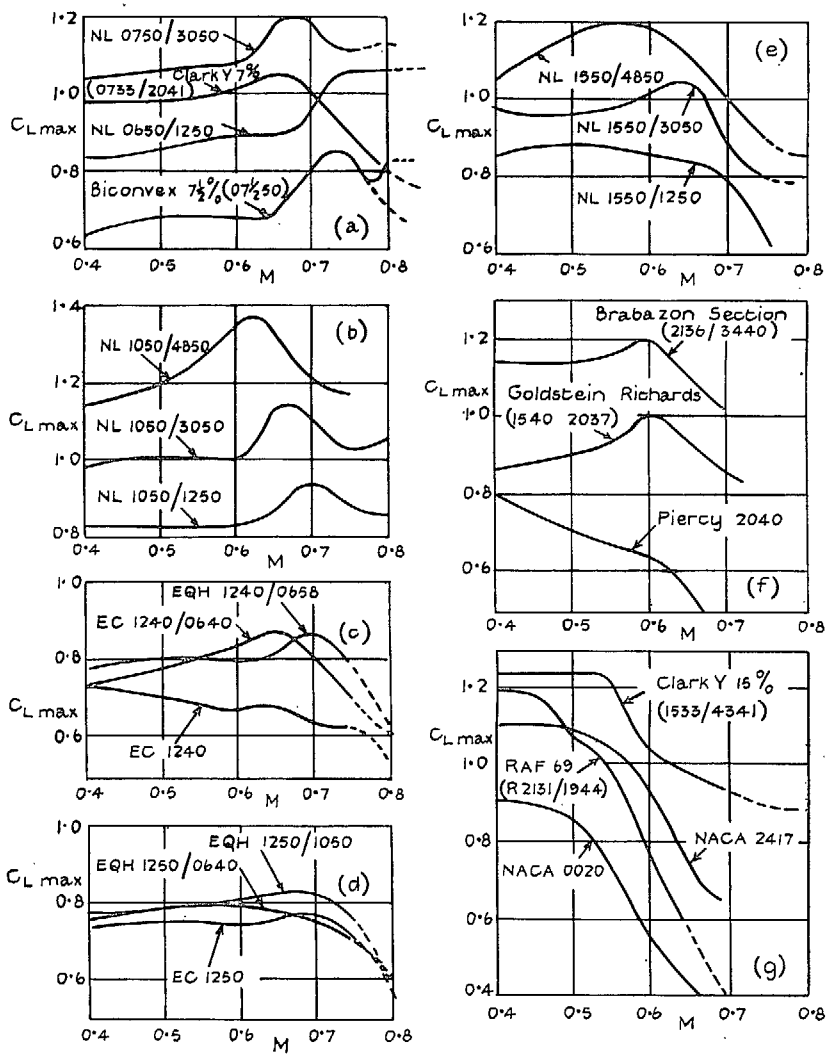

FIG. 35. Effect of camber.

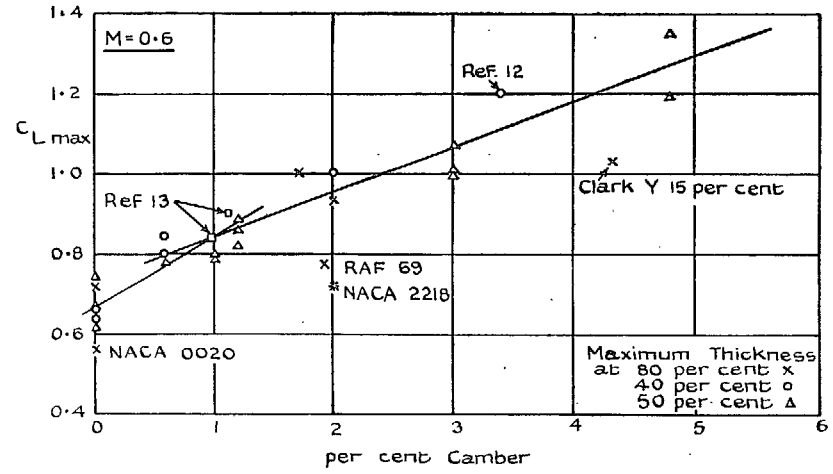

FIG. 36. Effect of camber at $M = 0{\cdot}6$.

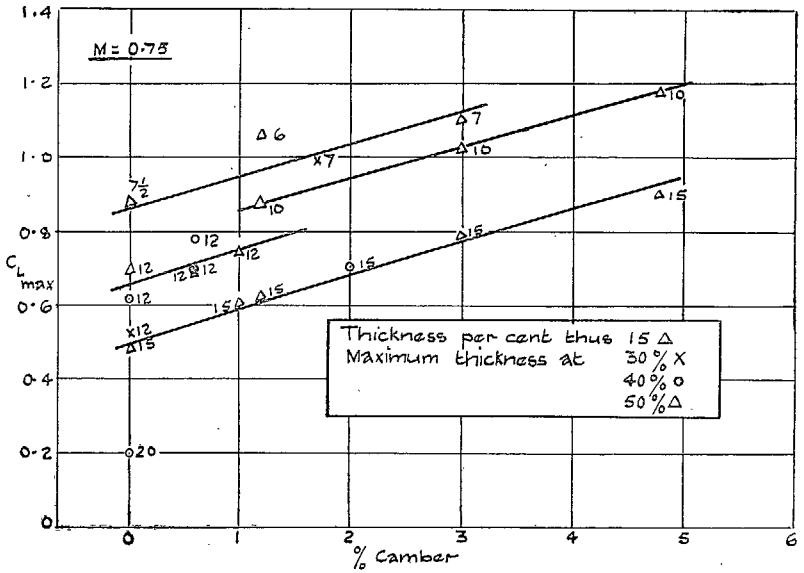

FIG. 37. Effect of camber and thickness at $M = 0{\cdot}75$.

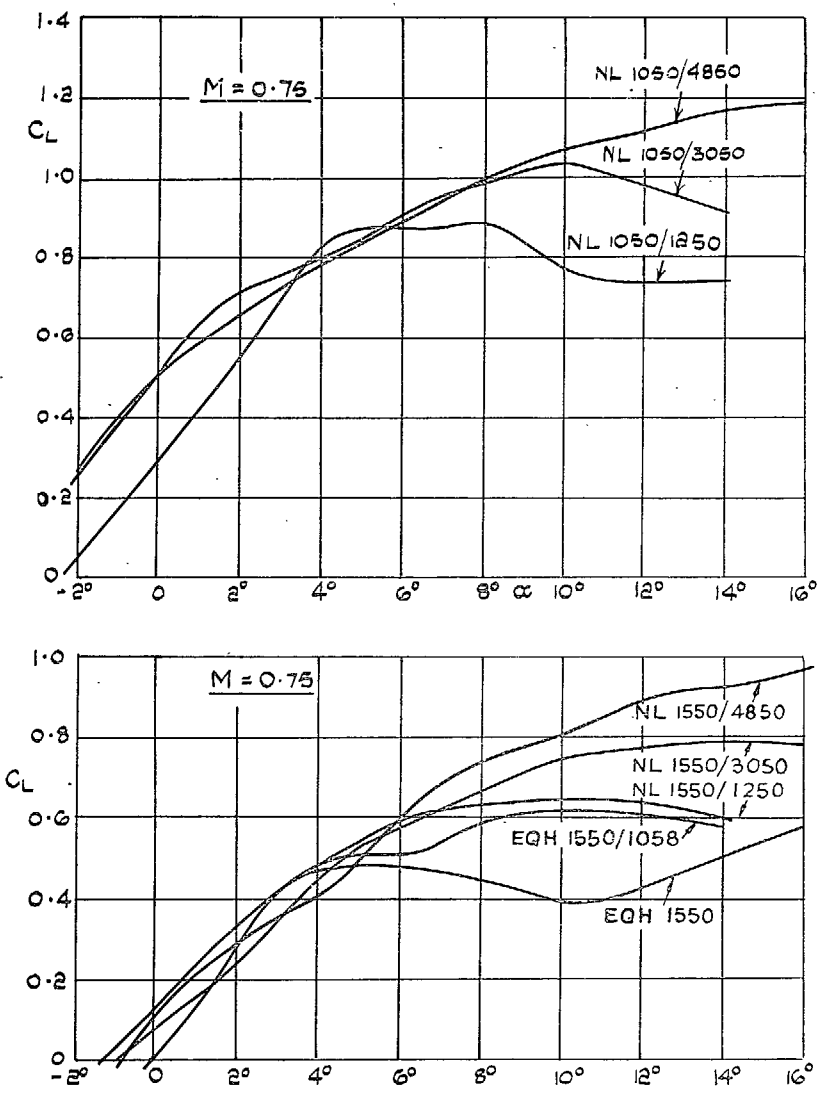

FIG. 38. Camber effect at high M.

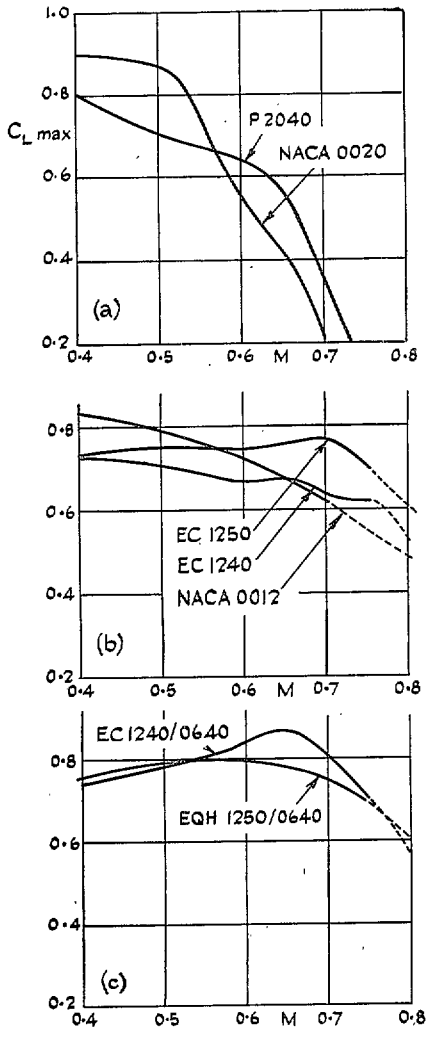

FIG. 39. Effect of thickness position.

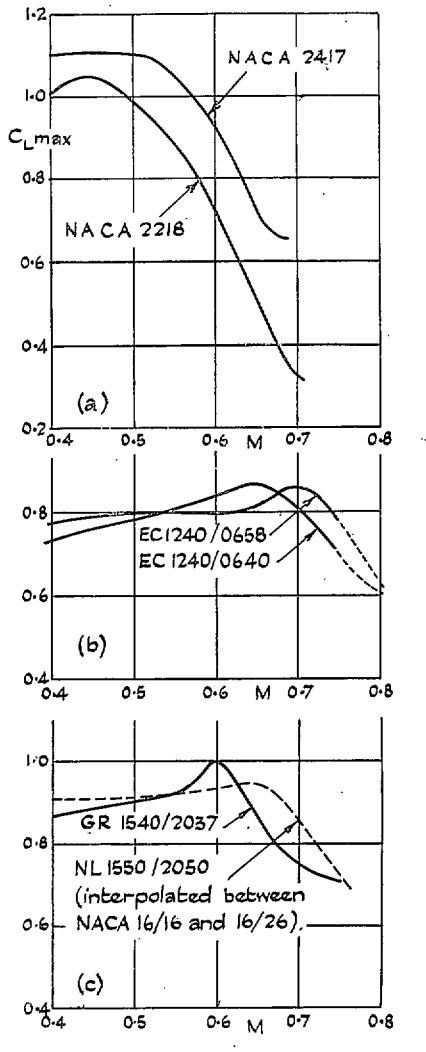

FIG. 40. Effect of camber position.

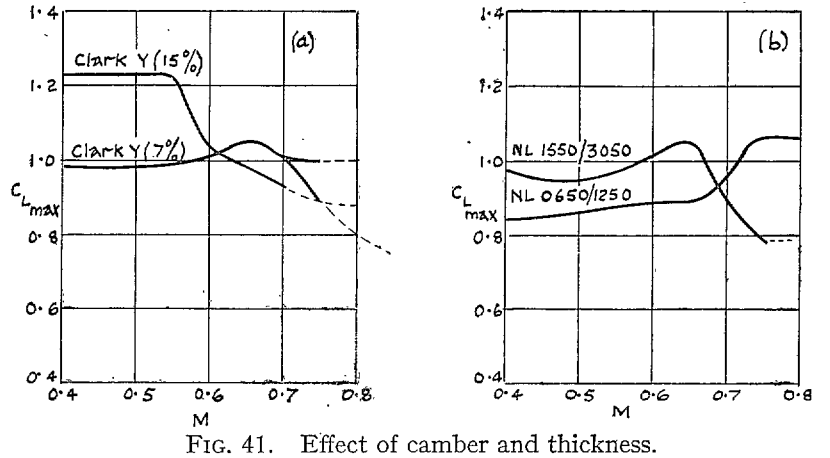

FIG. 41. Effect of camber and thickness.

(22734) Wt. 15-680 K9 4/53 F. M. & S. PRINTED IN GREAT BRITAIN

Publications of the Aeronautical Research Council

ANNUAL TECHNICAL REPORTS OF THE AERONAUTICAL RESEARCH COUNCIL (BOUND VOLUMES)

1936 Vol. I. Aerodynamics General, Performance, Airscrews, Flutter and Spinning. 40*s.* (40*s.* 9*d.*)
Vol. II. Stability and Control, Structures, Seaplanes, Engines, etc. 50*s.* (50*s.* 10*d.*)

1937 Vol. I. Aerodynamics General, Performance, Airscrews, Flutter and Spinning. 40*s.* (40*s.* 10*d.*)
Vol. II. Stability and Control, Structures, Seaplanes, Engines, etc. 60*s.* (61*s.*)

1938 Vol. I. Aerodynamics General, Performance, Airscrews. 50*s.* (51*s.*)
Vol. II. Stability and Control, Flutter, Structures, Seaplanes, Wind Tunnels, Materials. 30*s.* (30*s.* 9*d.*)

1939 Vol. I. Aerodynamics General, Performance, Airscrews, Engines. 50*s.* (50*s.* 11*d.*)
Vol. II. Stability and Control, Flutter and Vibration, Instruments, Structures, Seaplanes, etc. 63*s.* (64*s.* 2*d.*)

1940 Aero and Hydrodynamics, Aerofoils, Airscrews, Engines, Flutter, Icing, Stability and Control, Structures, and a miscellaneous section. 50*s.* (51*s.*)

1941 Aero and Hydrodynamics, Aerofoils, Airscrews, Engines, Flutter, Stability and Control, Structures. 63*s.* (64*s.* 2*d.*)

1942 Vol. I. Aero and Hydrodynamics, Aerofoils, Airscrews, Engines. 75*s.* (76*s.* 3*d.*)
Vol. II. Noise, Parachutes, Stability and Control, Structures, Vibration, Wind Tunnels. 47*s.* 6*d.* (48*s.* 5*d.*)

1943 Vol. I. (In the press.)
Vol. II. (In the press.)

ANNUAL REPORTS OF THE AERONAUTICAL RESEARCH COUNCIL—

1933-34	1*s.* 6*d.* (1*s.* 8*d.*)	1937	2*s.* (2*s.* 2*d.*)
1934-35	1*s.* 6*d.* (1*s.* 8*d.*)	1938	1*s.* 6*d.* (1*s.* 8*d.*)
April 1, 1935 to Dec. 31, 1936.	4*s.* (4*s.* 4*d.*)	1939-48	3*s.* (3*s.* 2*d.*)

INDEX TO ALL REPORTS AND MEMORANDA PUBLISHED IN THE ANNUAL TECHNICAL REPORTS AND SEPARATELY—

April, 1950 - - - - - R. & M. No. 2600. 2*s.* 6*d.* (2*s.* 7½*d.*)

AUTHOR INDEX TO ALL REPORTS AND MEMORANDA OF THE AERONAUTICAL RESEARCH COUNCIL—

1909-1949 - - - - - R. & M. No. 2570. 15*s.* (15*s.* 3*d.*)

INDEXES TO THE TECHNICAL REPORTS OF THE AERONAUTICAL RESEARCH COUNCIL—

December 1, 1936—June 30, 1939.	R. & M. No. 1850.	1*s.* 3*d.* (1*s.* 4½*d.*)
July 1, 1939—June 30, 1945.	R. & M. No. 1950.	1*s.* (1*s.* 1½*d.*)
July 1, 1945—June 30, 1946.	R. & M. No. 2050.	1*s.* (1*s.* 1½*d.*)
July 1, 1946—December 31, 1946.	R. & M. No. 2150.	1*s.* 3*d.* (1*s.* 4½*d.*)
January 1, 1947—June 30, 1947.	R. & M. No. 2250.	1*s.* 3*d.* (1*s.* 4½*d.*)
July, 1951. - - - - -	R. & M. No. 2350.	1*s.* 9*d.* (1*s.* 10½*d.*)

Prices in brackets include postage.

Obtainable from

HER MAJESTY'S STATIONERY OFFICE

York House, Kingsway, London, W.C.2; 423 Oxford Street, London, W.1 (Post Orders: P.O. Box 569, London, S.E.1); 13a Castle Street, Edinburgh 2; 39 King Street, Manchester 2; 2 Edmund Street, Birmingham 3; 1 St. Andrew's Crescent, Cardiff; Tower Lane, Bristol 1; 80 Chichester Street, Belfast or through any bookseller.